

THROMBOSIS AND HEMOSTASIS

S100A8/A9 drives the formation of procoagulant platelets through GPIb α

Martina Colicchia,¹ Waltraud C. Schrottmaier,² Gina Perrella,^{1,3} Jasmeet S. Reyat,¹ Jenefer Begum,¹ Alexandre Slater,¹ Joshua Price,⁴ Joanne C. Clark,¹ Zhaogong Zhi,¹ Megan J. Simpson,⁵ Joshua H. Bourne,¹ Natalie S. Poulter,^{1,6} Abdullah O. Khan,¹ Phillip L. R. Nicolson,^{1,7} Matthew Pugh,⁸ Paul Harrison,⁴ Asif J. Iqbal,¹ George E. Rainger,¹ Steve P. Watson,^{1,6} Mark R. Thomas,¹ Nicola J. Mutch,⁵ Alice Assinger,² and Julie Rayes^{1,6}

¹Institute of Cardiovascular Sciences, College of Medical and Dental Sciences, University of Birmingham, Birmingham, United Kingdom; ²Center for Physiology and Pharmacology, Medical University of Vienna, Vienna, Austria; ³Department of Biochemistry, CARIM, Maastricht University, Maastricht, The Netherlands; ⁴Institute of Inflammation and Ageing, University of Birmingham, Birmingham, United Kingdom; ⁵Aberdeen Cardiovascular & Diabetes Centre, Institute of Medical Sciences, School of Medicine, Medical Sciences and Nutrition, University of Aberdeen, Aberdeen, United Kingdom; ⁶Centre of Membrane Proteins and Receptors (COMPARE), Universities of Birmingham and Nottingham, The Midlands, United Kingdom; ⁷Department of Haematology, Queen Elizabeth Hospital, Birmingham, United Kingdom; and ⁸Institute of Immunology and Immunotherapy, University of Birmingham, Birmingham, United Kingdom

KEY POINTS

- S100A8/A9 plasma levels are increased in patients with COVID-19, and sustained high levels are associated with worse clinical outcome.
- S100A8/A9 induces the formation of procoagulant platelets through GPIb α supporting fibrin generation and immune-driven thrombosis.

S100A8/A9, also known as “calprotectin” or “MRP8/14,” is an alarmin primarily secreted by activated myeloid cells with antimicrobial, proinflammatory, and prothrombotic properties. Increased plasma levels of S100A8/A9 in thrombo-inflammatory diseases are associated with thrombotic complications. We assessed the presence of S100A8/A9 in the plasma and lung autopsies from patients with COVID-19 and investigated the molecular mechanism by which S100A8/A9 affects platelet function and thrombosis. S100A8/A9 plasma levels were increased in patients with COVID-19 and sustained high levels during hospitalization correlated with poor outcomes. Heterodimeric S100A8/A9 was mainly detected in neutrophils and deposited on the vessel wall in COVID-19 lung autopsies. Immobilization of S100A8/A9 with collagen accelerated the formation of a fibrin-rich network after perfusion of recalcified blood at venous shear. In vitro, platelets adhered and partially spread on S100A8/A9, leading to the formation of distinct populations of either P-selectin or phosphatidylserine (PS)-positive platelets. By using washed platelets, soluble S100A8/A9 induced PS exposure but failed to induce platelet aggregation, despite GPIIb/IIIa activation and alpha-granule secretion. We identified GPIb α as the

receptor for S100A8/A9 on platelets inducing the formation of procoagulant platelets with a supporting role for CD36. The effect of S100A8/A9 on platelets was abolished by recombinant GPIb α ectodomain, platelets from a patient with Bernard-Soulier syndrome with GPIb-IX-V deficiency, and platelets from mice deficient in the extracellular domain of GPIb α . We identified the S100A8/A9-GPIb α axis as a novel targetable prothrombotic pathway inducing procoagulant platelets and fibrin formation, in particular in diseases associated with high levels of S100A8/A9, such as COVID-19.

Introduction

Platelets are crucial for hemostasis and are key drivers of pathogenic thrombosis both in sterile and infectious conditions.^{1,2} Circulating activated platelets and platelet-leukocyte aggregates are increased in acute and chronic sterile thromboinflammatory diseases such as atherosclerosis,³ deep vein thrombosis (DVT),⁴ ischemic stroke,⁵ myocardial infarction (MI),^{6,7} and in infectious conditions such as sepsis,⁸ influenza,⁹ and COVID-19,¹⁰ with the increase in these levels correlating with disease severity.¹¹⁻¹³ Moreover, procoagulant platelets

and microvesicles (MVs), which support fibrin generation independent of platelet aggregation, are observed in trauma,¹⁴ COVID-19,¹⁵ coronary artery disease,^{16,17} sepsis,^{18,19} DVT, and stroke,²⁰⁻²² but the mechanisms triggering their formation are not well known.

Activation of neutrophils and neutrophil extracellular traps formation (NETosis) lead to the release of damage-associated molecular patterns (DAMPs) such as histones, myeloperoxidase (MPO), and S100A8/A9, which can promote inflammation and thrombosis.^{23,24} Recent work has demonstrated that

plasma levels of S100A8/A9, also known as “calprotectin” or “myeloid-related protein 8/14 (MRP-8/14)” are elevated in patients with COVID-19 and correlate with disease severity as well as thrombotic complications.²⁵⁻²⁹ High S100A8/A9 levels are also observed in MI,³⁰⁻³² sepsis,³³ and DVT,³⁴ with S100A8/A9 being used as a biomarker for immune cell activation and inflammation.³⁵⁻³⁷ S100A8 and S100A9 proteins belong to the 24 members of the multifunctional S100 family of cytoplasmic EF-hand helix-loop-helix Ca²⁺-binding proteins which regulate Ca²⁺ balance, cell apoptosis, migration, proliferation, differentiation, energy metabolism, and inflammation.³⁸ Extracellular S100A8 and S100A9 and the heterodimer S100A8/A9 promote inflammation and endothelial activation.³⁹ The heterodimer S100A8/A9 is the predominant form, comprising up to 45% and ~5% of all cytosolic proteins in neutrophils and monocytes, respectively.^{38,40,41} Three receptors have been described to mediate S100A8/A9 proinflammatory functions: the receptor for advanced glycation end products (RAGE), toll-like receptor-4 (TLR4), and the scavenger receptor CD36, which are expressed on different cells including platelets, immune cells, and endothelial cells.⁴²⁻⁴⁵ Innate immune cell activation leads to the release of S100A8/A9 and its deposition on venules, supporting leukocyte recruitment and transmigration.²⁹ Moreover, S100A8/A9 was shown to bind to heparan sulfate glycosaminoglycans on endothelial cells⁴⁶ and to induce endothelial activation through CD36⁴⁷ and RAGE.³⁹ Therefore, both soluble and immobilized S100A8/A9 may contribute to inflammation and thrombosis,^{27,34} with multiple receptors and mechanisms involved in thromboinflammatory diseases. We investigated the function of extracellular S100A8/A9 as a DAMP regulating platelet function and thrombosis. We show that S100A8/A9 induces the formation of procoagulant platelets through GPIIb α , independently of the known receptors for S100A8/A9, TLR4, and RAGE. CD36 blockage partially reduced GPIIb/IIIa activation and phosphatidylserine (PS) exposure on platelets without alteration in P-selectin expression. We have identified the S100A8/A9-GPIIb α axis as a novel prothrombotic pathway that triggers the formation of procoagulant platelets accelerating fibrin generation and thrombosis.

Materials and methods

Ethical approval

Ethical approval for collecting blood from healthy volunteers was granted by Birmingham University Internal Ethical Review (ERN_11-0175). Mouse experiments were performed in accordance with UK laws (Animal [Scientific Procedures] Act 1986) with approval of the local ethical committee and UK Home Office approval (PPL Pp9677279). Ethical approval for collecting postmortem tissues was granted by the North-East — Newcastle & North Tyneside 1 Research Ethics Committee (19/NE/0336). Collection of postmortem formalin-fixed and paraffin-embedded tissue was approved (IRAS: 197937) for tissue obtained via prospective consent postmortem and retrospective acquisition of tissue in which consent for use in research had already been obtained. Ethics for patient tissue were approved by the Health Research Authority with a National Health Service Research Ethics Committee. All necessary patient/participant written consent has been obtained, and the appropriate institutional forms have been archived. This research adheres to the tenets of the Declaration of Helsinki. Blood from patients with COVID-19 was collected under the ethical approval of Medical

University of Vienna (EK1315/2020) as part of the Austrian Coronavirus Adaptive Clinical Trial (ACOVACT; [ClinicalTrials.gov](https://clinicaltrials.gov/NCT04351724) NCT04351724).

Plasma S100A8/A9 enzyme-linked immunosorbent assay (ELISA)

Plasma was collected by blood centrifugation for 10 minutes at 1000g (4°C) followed by 10 minutes of centrifugation at 10.000g at room temperature.⁴⁸ Plasma samples were stored at –80°C until use. Plasma levels of S100A8/A9 were measured using LEGEND MAX Human MRP8/14 (Calprotectin) ELISA Kit (BioLegend).

Immunofluorescence staining of lung sections

Human paraffin-embedded lung sections (6 μ m) were processed and stained as previously described.⁴⁹ Antibodies against platelet CD42b, MPO, fibrin, S100A8/A9, and S100A9 (supplemental Table 1, available on the *Blood* website) were incubated overnight at 4°C followed by secondary conjugated antibodies. Lung autofluorescence was quenched using a commercial kit (Vector Laboratories) and slides mounted using ProLong Gold Antifade Mountant (Life Technologies). Sections were imaged using an Epifluorescent microscope or Zeiss AxioScan Z1 microscope and analyzed using ZEN software and ImageJ.

Recombinant S100A8/A9 production and purification

Commercial recombinant S100A8/A9 (BioLegend) and in-house-produced proteins were used. Recombinant human heterodimeric S100A8/A9 was produced as previously described with minor changes.⁵⁰ Protein production and purification are detailed in the supplemental Data.

Platelet preparation and functional assays

Human and mouse blood were collected in sodium citrate and ACD-A Anticoagulant Citrate Dextrose solution, respectively, as previously described.^{51,52} Platelet preparation and functional assays (platelet aggregation and ATP generation, thrombin generation test, flow adhesion assay, platelet spreading, intracellular Ca²⁺ release) are detailed in the supplemental Data.

Data analysis

All data were presented as mean \pm standard deviation (SD) unless stated otherwise. The logarithmic dose-binding curves were generated through 4-parameter nonlinear regression analysis with variable slopes. The statistical difference between groups was analyzed using either one-way or two-way analysis of variance (ANOVA) with multiple comparisons or Kruskal-Wallis test with multiple comparisons or as stated in the legends for [Figures 1, 5, and 6](#) using Prism 7 (GraphPad Software Inc).

Results

Sustained high levels of S100A8/A9 in the plasma of patients with COVID-19 correlate with adverse outcome

Plasma S100A8/A9 levels are elevated in patients with COVID-19 and these levels correlate with thrombosis.^{28,53,54} In a cohort of 87 patients with COVID-19,^{55,56} plasma levels of S100A8/A9

were measured by ELISA over the first week of study enrollment. Study inclusion occurred up to 72 hours after hospital admission. Patients were stratified on the basis of the clinical severity into uncomplicated (not requiring intensive care treatment) and complicated (intensive care unit [ICU] survivors and nonsurvivors). At study recruitment, the levels of S100A8/A9 were elevated in the plasma of all patients with COVID-19 compared with healthy controls (Figure 1A). Over the first 7 days of monitoring, the levels of S100A8/A9 remained high in patients with complicated COVID-19 but decreased in uncomplicated patients (Figure 1B-C). The levels of S100A8/A9 were significantly higher in nonsurvivors ranging between 10 and 40 $\mu\text{g/mL}$. These data show that sustained high levels of plasma S100A8/A9 correlated with COVID-19 disease severity.

Heterodimeric S100A8/A9 is detected in neutrophils and on the lung vessel walls of patients with COVID-19

S100A8/A9 release from activated immune cells leads to deposition on venule endothelial cells, supporting leukocyte recruitment and transmigration.²⁹ The presence and location of S100A8/A9 were assessed in lung autopsies from COVID-19 nonsurvivor patients ($n = 8$)⁴⁹ and control sections from age-matched patients ($n = 3$). By using an antibody recognizing the heterodimer S100A8/A9 but not S100A8 or S100A9 alone, S100A8/A9 was detected in neutrophils (MPO-positive cells) and on the vessel wall (Figure 1D-E). S100A8/A9 was also detected in a fraction of CD42b-positive cells in patients with COVID-19 but not in controls. Platelets were observed lining the endothelium as single platelets, as small aggregates positive for S100A9 and fibrin, or were integrated into large fibrin-rich thrombi (Figure 1D,F-G). Contrary to the antibody recognizing the dimeric form, staining with anti-S100A9 antibody revealed a strong colocalization between CD42b and S100A9 in COVID-19 lungs (Figure 1G). These results show an increase in soluble S100A8/A9 alongside its deposition on the vasculature in COVID-19 lungs.

Immobilized S100A8/A9 supports fibrin generation at venous shear rate

Platelet-derived S100A8/A9 was shown to promote thrombosis partially via CD36.²⁷ Platelets from patients with COVID-19 are enriched in S100A8/A9 and platelet releasate induces endothelial cell activation via CD36²⁸ but the effect of extracellular S100A8/A9 on platelets is not well known. We assessed the effect of soluble and immobilized recombinant S100A8/A9 on fibrin generation in whole blood from healthy donors. Commercial and in-house-produced recombinant S100A8/A9 were used and characterized (supplemental Figure 1A-D). Both proteins are heterodimers and the S100A9 protein is phosphorylated at Thr113, which is essential for the proinflammatory functions of extracellular S100A8/A9⁵⁷ (supplemental Figure 1A-D). S100A8/A9 induces the secretion of tumor necrosis factor (TNF)- α from human monocytes in a TLR4-dependent manner as TAK-242 significantly reduced TNF- α levels in monocyte supernatant, showing the functionality of in-house-produced S100A8/A9 (supplemental Figure 1E). Addition of S100A8/A9 in platelet-rich plasma (PRP) isolated from healthy donors did not support thrombin generation in calibrated automated thrombography compared with PRP alone (supplemental Figure 2A-F). However, perfusion of whole blood over S100A8/A9-coated surfaces under recalcified

conditions at venous shear rate (100 s^{-1}), induced platelet adhesion with local fibrin generation as assessed using anti-fibrin/fibrinogen antibody and early recruitment of PS-positive platelets detected by annexin-V binding (Figure 1H-J). Compared with S100A8/A9 or collagen alone, surface coated with S100A8/A9 in combination with collagen accelerated the recruitment of annexin-V-positive platelets and the formation of multiple fibrin-rich areas and widespread fibrin network, which significantly limited blood flow (Figure 1H-J). These results indicate that immobilized S100A8/A9 accelerates the formation of fibrin-rich thrombi at venous shear.

Recombinant S100A8/A9 induces human platelet activation without aggregation in vitro

It has been recently shown that arterial and venous thrombus formation was reduced in mice deficient in S100A8/A9.^{27,34} To identify whether S100A8/A9 exerts a direct effect on platelets leading to pathogenic thrombosis, we assessed the effect of recombinant S100A8/A9 on platelet function in vitro. The incubation of human washed platelets with increasing concentrations of S100A8/A9 at ranges previously detected in thromboinflammatory diseases and COVID-19 patients^{26,33,53,58,59} induced platelet activation as assessed by flow cytometry (Figure 2). S100A8/A9 induced a slow release of P-selectin from alpha-granules as measured using an anti-P-selectin antibody (Figure 2A-B, supplemental Figure 2G). Platelet activation by S100A8/A9 was not homogenous among healthy donors, with high responders reaching similar levels of platelet activation as for collagen-related peptide (CRP) and thrombin receptor-activating peptide 6 (TRAP-6), even at low doses of S100A8/A9 (10-20 $\mu\text{g/mL}$) (Figure 2B). The upregulation in P-selectin expression was associated with increased platelet-neutrophil aggregates in diluted whole blood after stimulation with S100A8/A9 (Figure 2C). S100A8/A9 induced GPIIb/IIIa activation as assessed by the binding of an anti-CD61/CD41 PAC-1 antibody, which recognizes the activated form of the integrin (Figure 2D). GPIIb/IIIa activation occurred quickly after the addition of S100A8/A9 compared with the slow upregulation of P-selectin (supplemental Figure 2H). Surprisingly, despite GPIIb/IIIa activation, S100A8/A9 did not induce platelet aggregation (Figure 2E-F) as assessed by light transmission aggregometry or dense granule release (Figure 2G-H). S100A8/A9 did not induce platelet aggregation in the presence of exogenous fibrinogen, suggesting that the absence of aggregation is not due to a defect in fibrinogen secretion but possibly an alteration in fibrinogen binding (Figure 2I-J). Indeed, addition of exogenous labeled fibrinogen to platelets in the presence of S100A8/A9 showed low binding capacity compared with CRP (Figure 2K-L). These results indicate that S100A8/A9 induces P-selectin upregulation and GPIIb/IIIa activation without platelet aggregation, suggesting a novel mechanism of platelet activation independent of platelet aggregation.

S100A8/A9 induces PS exposure on platelets and the release of PS-positive MVs

Procoagulant platelets, which expose high levels of PS, have a very low capacity to aggregate with some procoagulant platelet populations sustaining the active form of GPIIb/IIIa.⁶⁰ Therefore, surface expression of PS on S100A8/A9-activated platelets was assessed by annexin-V binding using flow cytometry. S100A8/A9 induced PS exposure on the surface of platelets (Figure 3A-C), which occurred

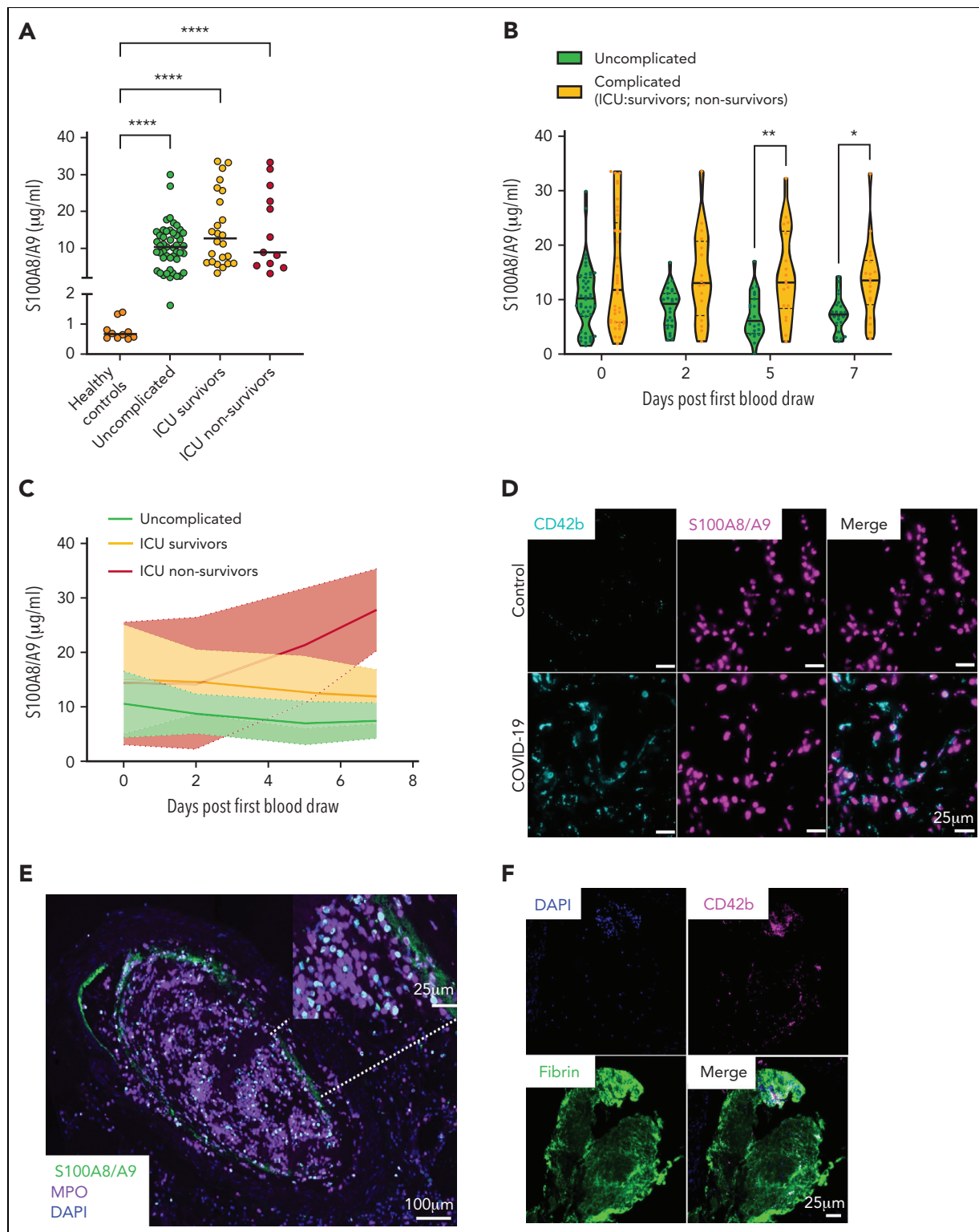


Figure 1. S100A8/A9 accelerates the recruitment of annexin-V-positive platelets and fibrin generation at a venous shear rate. (A-C) Plasma levels of S100A8/A9 were measured by ELISA in healthy donors and patients with uncomplicated and complicated (ICU survivors/nonsurvivors) COVID-19 over 7 consecutive days after inclusion in the study. (A) S100A8/A9 levels in the plasma of healthy donors (control, $n = 10$), uncomplicated COVID-19 patients ($n = 48$), ICU survivors ($n = 26$), and ICU nonsurvivors ($n = 13$) on the first day of patient inclusion in the study. (B-C) S100A8/A9 levels in the plasma over 7 consecutive days after patient recruitment. (D-G) Representative immunofluorescence staining of lung autopsies obtained from COVID-19 patients or age-matched control. Images were captured using Epi fluorescence microscope and slide scanner Axioscan Z1. (D) Platelet CD42b and heterodimeric S100A8/A9 staining in lung parenchyma and microcirculation in COVID-19 and control lung autopsies. (E) Staining for S100A8/A9, MPO, and nuclei (DAPI) of a large vessel in the lung of a patient with COVID-19 with thrombotic complications. (F) Staining for platelet CD42b, fibrin, and nuclei (DAPI) in large thrombi of a patient with COVID-19. (G) S100A9, CD42b, and fibrin staining in COVID-19 lung. Arrow shows platelet-fibrin microaggregates. (H) Whole blood under recalcified conditions was perfused at a venous shear rate (100 s^{-1}) over S100A8/A9 (40 µg/mL), collagen (100 µg/mL), or combination of S100A8/A9 and collagen-coated chambers. The

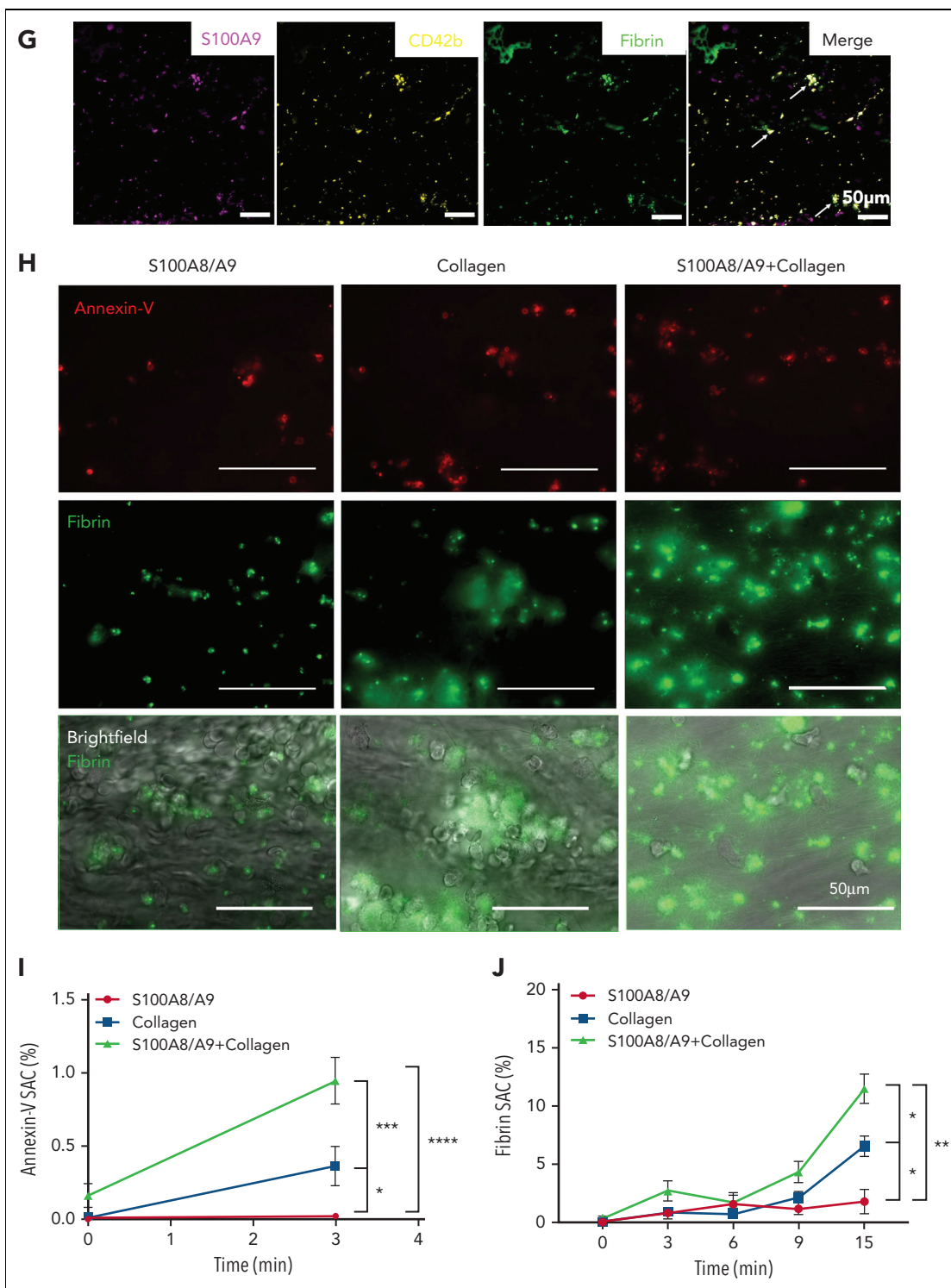


Figure 1 (continued) presence of PS-positive platelets and fibrin were assessed using annexin-V-Alexa Fluor-647 and FITC-anti-fibrinogen/fibrin antibody, respectively. (H) Representative images taken at 15 minutes. (I) Quantification of annexin-V signal (3 minutes) (n = 5) and (J) fibrin signal time course (0-15 minutes) (n = 5) using predefined semiautomated scripts in Fiji as detailed in the supplemental Methods (available on the *Blood* website). Results are shown as mean \pm standard error of the mean (SEM). The statistical significance was analyzed using two-way ANOVA with Tukey's multiple comparison test between all groups. * $P < .05$, ** $P < .005$, *** $P < .001$, **** $P < .0001$.

rapidly after the addition of S100A8/A9 (supplemental Figure 2I). S100A8/A9 also increased the level of PS on CD41-positive MVs (Figure 3D). Platelet activation is dependent on the presence of the heterodimer because recombinant S100A8 or S100A9 alone did not induce platelet activation

(supplemental Figure 2J-L). Platelets adhered to and spread on immobilized S100A8/A9, whereas no significant platelet adhesion was observed on bovine serum albumin used as negative control (Figure 3E). Platelet adhesion on immobilized S100A8/A9 showed predominantly high expression of either PS or P-selectin

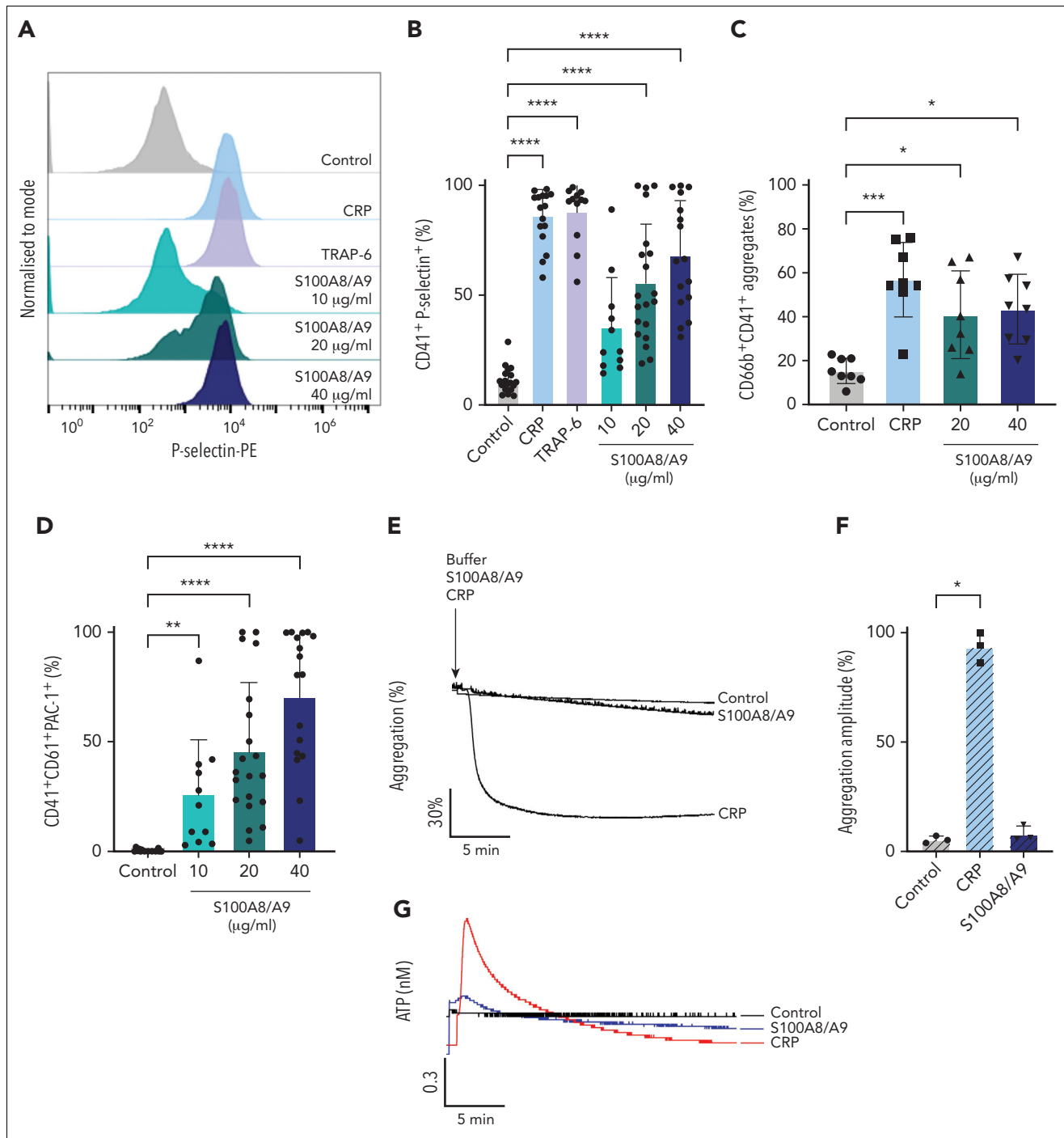


Figure 2. Recombinant S100A8/A9 induces human platelet activation in vitro. Human washed platelets (10^6 platelets/condition) were incubated with different concentrations of recombinant heterodimeric S100A8/A9 (10, 20, and 40 $\mu\text{g}/\text{mL}$) for 30 minutes at 37°C . (A-B) Platelet activation was determined by flow cytometry using anti-P-selectin antibody. (A) Representative plots from a healthy donor; histograms normalized to mode (each peak normalized to its mode for each condition). (B) Percentage of $\text{CD41}^+\text{P-selectin}^+$ platelets. (C) The percentage of platelet-neutrophil aggregates ($\text{CD66b}^+/\text{CD41}^+$) in whole blood after addition of S100A8/A9 for 30 minutes at 37°C ($n = 7$). Blood was diluted 1:5. (D) Anti- $\text{CD41}/\text{CD61}$ PAC-1 antibody (against activated GPIIb/IIIa) binding to platelets was assessed by flow cytometry and presented as percentage of CD41^+ platelets positive for PAC-1 ($n = 17$). (E-F) Washed platelets ($2 \times 10^8/\text{mL}$) were incubated with S100A8/A9 (40 $\mu\text{g}/\text{mL}$) or CRP (10 $\mu\text{g}/\text{mL}$), and platelet aggregation was assessed for 20 minutes by light transmission aggregometry ($n = 3$). (G-H) Washed platelets ($2 \times 10^8/\text{mL}$) were incubated with S100A8/A9 (40 $\mu\text{g}/\text{mL}$) or CRP (10 $\mu\text{g}/\text{mL}$), and ATP generation was assessed for 6 minutes with the CHRONO-LUME luciferin:luciferase assay kit from Chronolog ($n = 3$). (I-J) Washed platelets ($2 \times 10^8/\text{mL}$) were incubated with S100A8/A9 (20 $\mu\text{g}/\text{mL}$ or 40 $\mu\text{g}/\text{mL}$) for 6 minutes under stirring condition followed by the addition of exogenous fibrinogen (200 $\mu\text{g}/\text{mL}$). Platelet aggregation was assessed for 6 minutes by light transmission aggregometry ($n = 3$). (K-L) Alexa-Fluor 488-labeled fibrinogen binding to platelets. (K) Representative plot for fibrinogen binding. (L) Percentage of platelets positive for fibrinogen-Alexa Fluor 488, CRP (10 $\mu\text{g}/\text{mL}$) and TRAP-6 (100 μM) were used as positive control. Data are shown as mean \pm SD. The statistical significance was analyzed using ordinary one-way ANOVA. * $P < .05$, ** $P < .005$, *** $P < .001$, **** $P < .0001$.

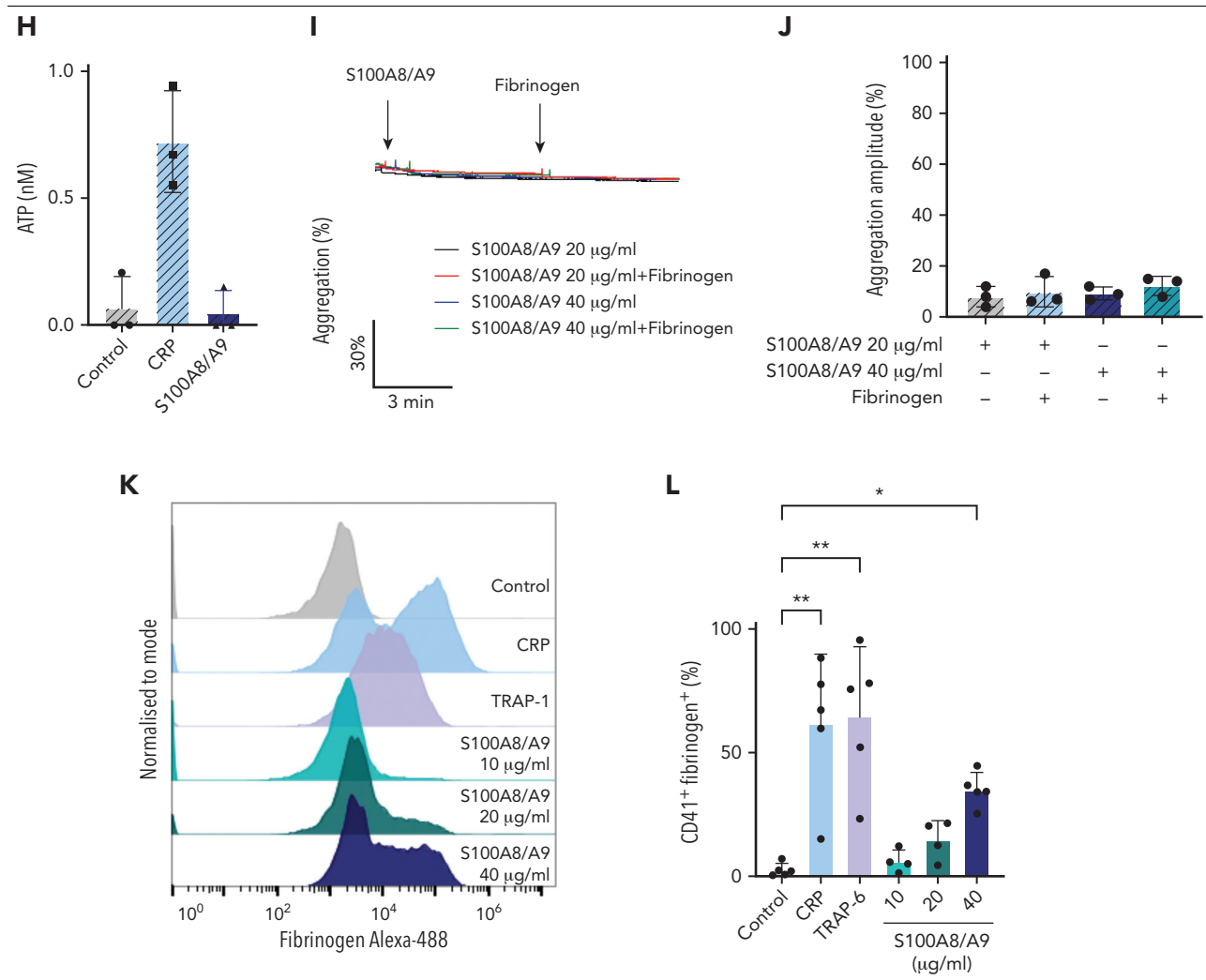


Figure 2. (continued)

on adherent platelets, with low expression of P-selectin on PS-positive platelets and vice versa (Figure 3F-G). Increasing the coating density of S100A8/A9 augmented the formation of PS-positive platelet and PS-positive MVs rather than P-selectin-positive platelets (Figure 3G). In addition, platelet adhesion on S100A8/A9 induced intracellular Ca²⁺ release (Figure 3H-I), with high Ca²⁺ signal observed in adherent but not spread platelets. These results indicate that S100A8/A9 induces intracellular Ca²⁺ release, PS exposure, and the release of PS-positive MVs, and that this activation is restricted to the heterodimeric form of S100A8/A9.

CD36 blockade and immunoreceptor tyrosine-based activation motif receptor inhibitors differentially reduce the effect of S100A8/A9 on platelets

S100A8/A9 has 3 known receptors (RAGE, TLR4, and CD36), which are all expressed on platelets.⁶¹⁻⁶³ To identify the functional receptor for S100A8/A9 mediating the formation of procoagulant and activated platelets, we first assessed the

effect of inhibitors targeting TLR4, RAGE, and CD36 in human washed platelets. Inhibition of RAGE using Azeliragon or S100A9 binding to TLR4 using Paquinimod did not alter platelet activation by S100A8/A9 (Figure 4A-C). Moreover, inhibition of TLR-4, using the small molecule inhibitor TAK-242 or an antibody inhibiting S100A8/A9 binding to TLR4 and RAGE (S100A8/A9 Ab clone A1505B), also did not alter platelet activation or PS exposure (supplemental Figure 3A-C, supplemental Table 2). Blocking downstream signaling of CD36 using sulfosuccinimidyl oleate (SSO), which irreversibly blocks CD36, partially reduced GPIIb/IIIa activation and PS exposure without affecting P-selectin expression (Figure 4D-F). An antibody that blocks the oxidized low-density lipoprotein binding site to CD36 (CD36 blocking Ab) had no effect on platelet activation, suggesting the presence of distinct binding sites for S100A8/A9 and oxidized low-density lipoprotein on CD36 (supplemental Figure 3D-E). Further, inhibition of platelet immunoreceptor tyrosine-based activation motif receptors using inhibitors for Src (PP2), Syk (PRT-060318), or Btk (ibrutinib) did not alter the binding of anti-CD61/CD41 PAC-1 antibody or annexin-V (Figure 4G-I), while significantly reducing P-selectin expression

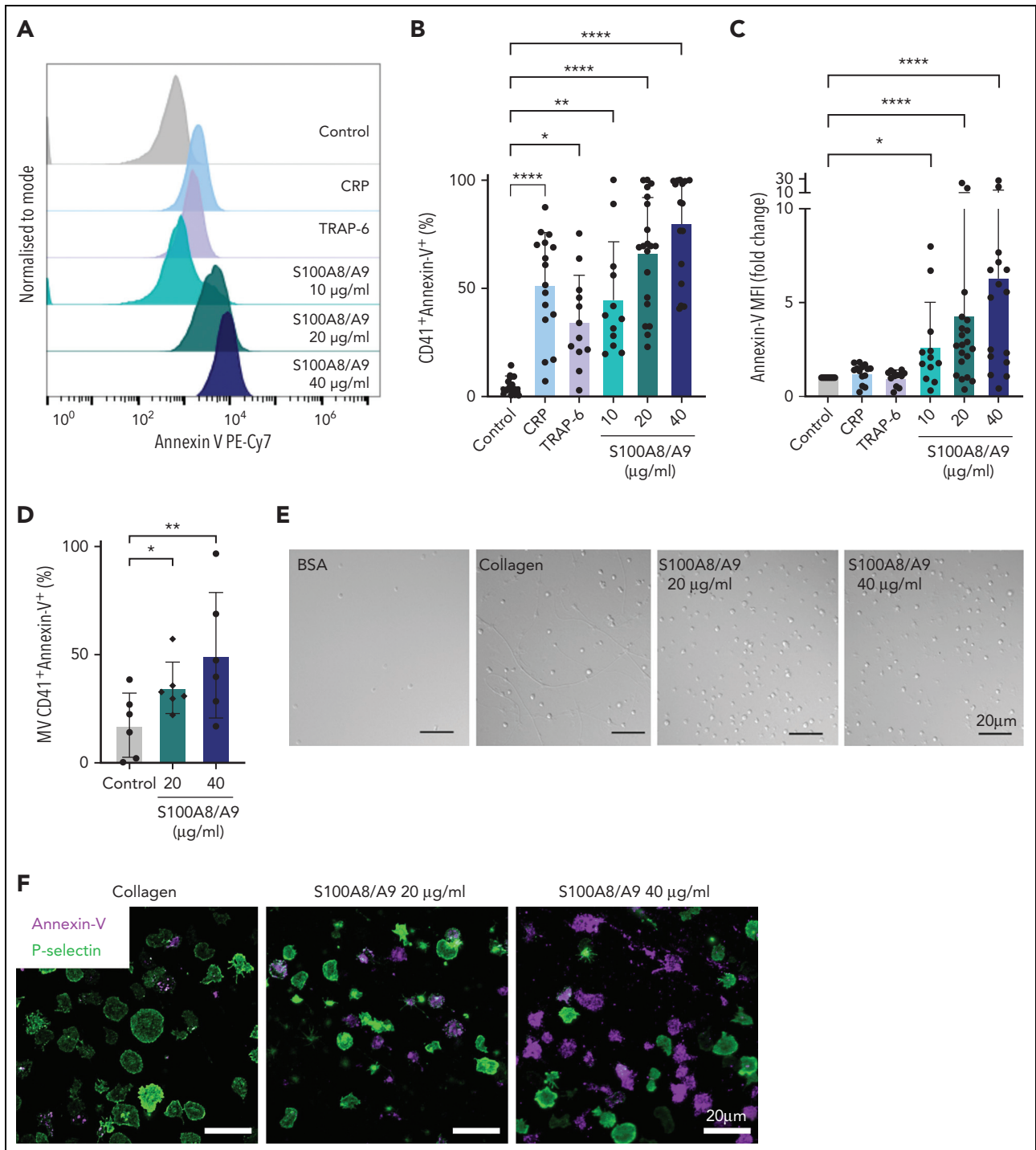


Figure 3. S100A8/A9 induces the formation of procoagulant platelets. Human washed platelets (10^6 platelets/condition) were incubated with different concentrations of S100A8/A9 (10, 20 and 40 µg/mL) for 30 minutes at 37°C. (A-C) PS exposure was determined by flow cytometry using PE-Cy7–labeled annexin-V ($n = 17$). CRP (10 µg/mL) and TRAP-6 (100 µM) were used as positive control. (A) Representative histogram for annexin-V staining. Representative histograms normalized to mode (each peak normalized to its mode for each condition). (B) Percentage of CD41⁺annexin-V⁺ platelets. (C) Fold change in the mean fluorescent intensity (MFI) of agonist-activated platelets over control. (D) The percentage of CD41⁺MVs positive for annexin-V ($n = 6$). (E-F) Human washed platelets spreading on collagen or S100A8/A9. Representative differential interference contrast (DIC) images of spread platelets. (F) Representative annexin-V (magenta) and P-selectin (green) staining for adherent platelets. (G) Quantification of annexin-V–positive, P-selectin–positive, or annexin-V and P-selectin–double positive platelets adherent on collagen and S100A8/A9 (positive platelets/total platelets). The statistical significance was analyzed using two-way ANOVA with Tukey’s multiple comparison test between all groups. (H-I) Assessment of intracellular Ca²⁺ release from platelets spread over surfaces coated with S100A8/A9 (20 and 40 µg/mL), fibrinogen, or bovine serum albumin assessed using BAPTA-1-AM Ca²⁺ sensitive dye. (H) Representative Ca²⁺ traces assessed using Oregon Green-488 BAPTA-1-AM. (I) Peak fluorescence at time point zero (F0/Fmax). Data are shown as mean ± SD. The statistical significance was analyzed using a nonparametric test (Kruskal-Wallis test). * $P < .05$, ** $P < .005$, *** $P < .001$, **** $P < .0001$.

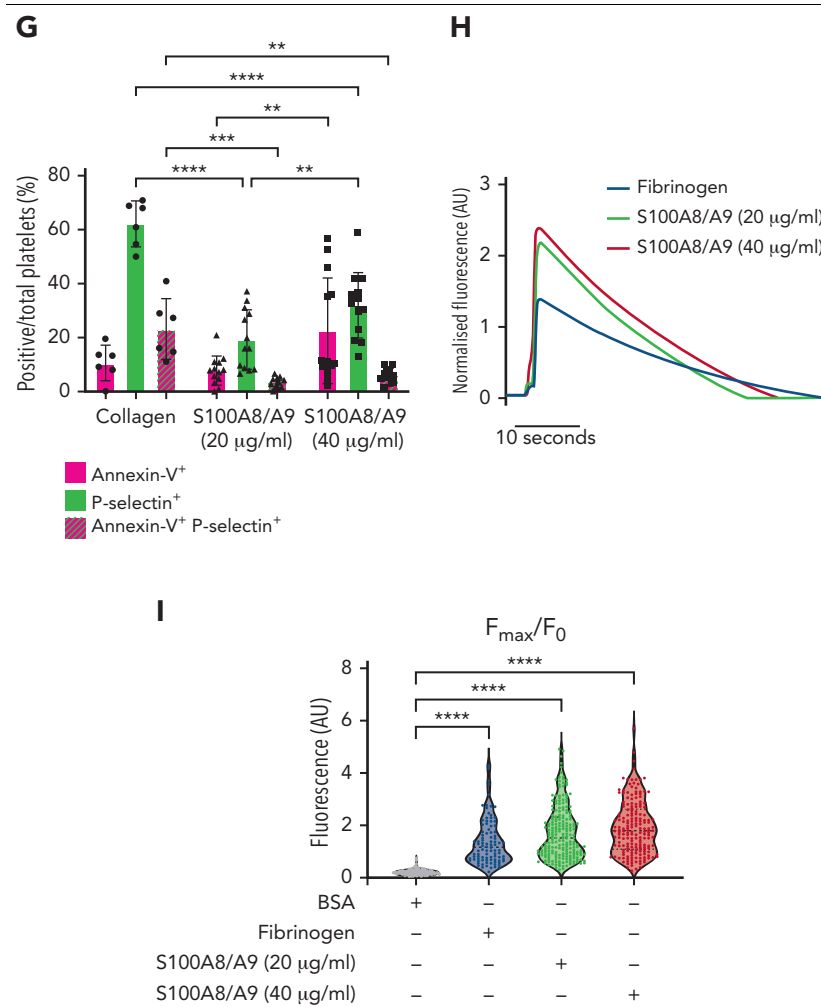


Figure 3. (continued)

on platelets (Figure 4H). Inhibition of Syk showed the highest inhibition of P-selectin expression, which was associated with a decrease in platelet-neutrophil aggregates in whole blood (supplemental Figure 3F). Inhibition of cyclo-oxygenase using indomethacin or P2Y12 using cangrelor did not alter platelet activation or PS exposure (supplemental Figure 3G-I). These results suggest that S100A8/A9-mediated P-selectin upregulation is regulated by Syk/Src, whereas GPIIb/IIIa activation and PS exposure are partially mediated through CD36.

Murine recombinant S100A8/A9 activates mouse platelets in a dose-dependent manner through GPIb α

As CLEC-2, GPVI, GPIb, and CD36 signal through Syk/Src,^{64,65} we assessed the effect of S100A8/A9 on murine platelets deficient in CLEC-2, GPVI, CLEC-2/GPVI, or platelets deficient in the extracellular domain of GPIb α (IL4R/GPIb α -Tg mice). Mouse S100A8/A9 induced the activation of wild-type (WT) platelets in a dose-dependent manner as assessed using anti-P-selectin antibody and annexin-V binding in a similar manner as in human platelets (Figure 5A-B). Deletion of GPVI, CLEC-2, or both receptors, did not significantly alter P-selectin expression or

annexin-V binding in response to S100A8/A9 compared with WT mice (Figure 5C-D). However, GPVI^{-/-} and GPVI^{-/-} CLEC-2^{-/-} mice showed a bimodal pattern for P-selectin expression. S100A8/A9-induced mouse platelet activation was significantly reduced in platelets deficient in the extracellular domain of GPIb α (IL4R/GPIb α -Tg) as measured by P-selectin expression (Figure 5E-F), annexin-V binding (Figure 5G-H), and GPIIb/IIIa activation (Figure 5I-J). Compared with GPIIb/IIIa activation in human platelets, mouse S100A8/A9 induced modest integrin activation (Figure 5I-J). The partial reduction in annexin-V binding observed in IL4R/GPIb α -Tg platelets was completely blocked by the addition of the CD36 inhibitor SSO (Figure 5K). Collectively, these results indicate that GPIb α and CD36 are putative receptors for S100A8/A9 on mouse platelets.

Recombinant human GPIb α binds to S100A8/A9 and potentiated von Willebrand factor (VWF)-mediated platelet agglutination

To assess whether GPIb α is the main receptor for S100A8/A9 on human platelets or indirectly regulates S100A8/A9-mediated platelet activation, direct binding between GPIb α and S100A8/A9 was assessed by ELISA. S100A8/A9 binds to recombinant

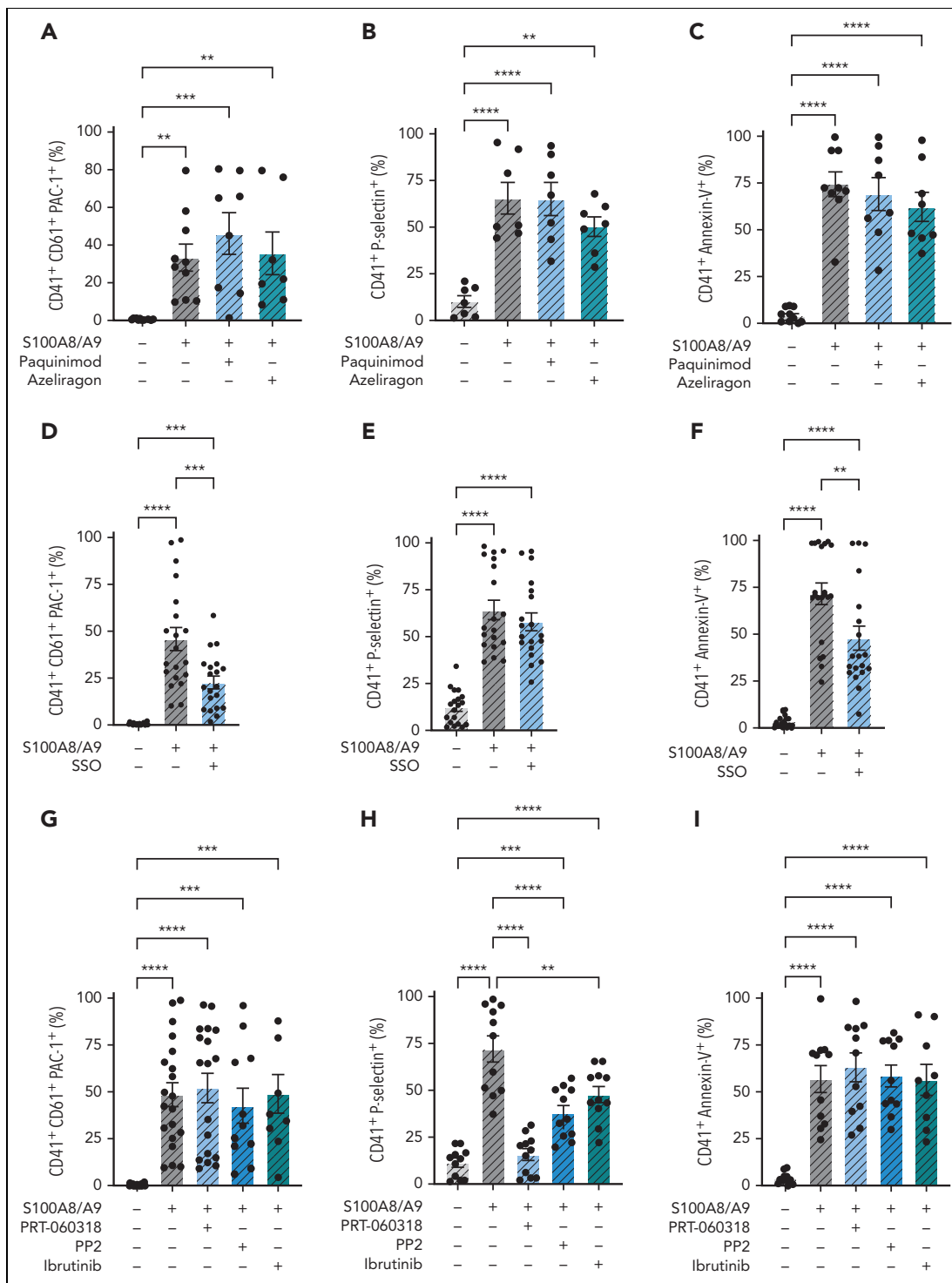


Figure 4. CD36 blockade partially decreases GPIIb/IIIa activation and PS exposure, whereas immunoreceptor tyrosine-based activation motif receptor inhibition reduces P-selectin expression. Human washed platelets (10^6 platelets/condition) were incubated with S100A8/A9 (20 μ g/mL) with or without different inhibitors for 30 minutes at 37°C. Inhibitors were preincubated with platelets for 10 minutes before addition of S100A8/A9: Paquinimod (blocks S100A9 binding to TLR4) (10 μ M), RAGE inhibitor Azeliragon (1 μ M), CD36 inhibitor SSO (25 μ M), Syk inhibitor PRT-060318 (10 μ M), Src inhibitor PP2 (20 μ M), and BTK inhibitor Ibrutinib (500 nM) were used. Platelet activation was determined by flow cytometry using (A,D,G) anti-CD41/CD61 PAC-1 antibody, (B,E,H) anti-P-selectin antibody, and (C,F,I) annexin-V binding. Data are shown as the percentage of platelets positive (CD41⁺) for these markers. Data are shown as mean \pm SD. Statistical significance was analyzed using ordinary one-way ANOVA. * $P < .05$, ** $P < .005$, *** $P < .001$, **** $P < .0001$.

GPIIb α with an EC₅₀ of 130 ± 75 nM (Figure 6A). Furthermore, the effect of anti-GPIIb α antibodies AK2, SZ2, and the peptide OS-1, which were previously described to block the interaction

of GPIIb α with VWF, on S100A8/A9-induced platelet activation was assessed as described above. SZ2 and AK2 antibodies, which recognize distinct epitopes on GPIIb α located within the

anionic/sulfated tyrosine region (Tyr2-Glu282) and in the first leucine-rich repeat (Leu36-Gln59), respectively, and OS-1 peptide, which allosterically inhibits GPIIb-IIIa interaction, were tested at concentrations previously shown to inhibit VWF-mediated platelet agglutination⁶⁶⁻⁶⁸ (supplemental Figure 4A-G, Figure 6B-D). AK2 and SZ2 significantly decreased PS exposure and GPIIb/IIIa activation, and this inhibition was further pronounced using a combination of both antibodies (Figure 6B-D, supplemental Figure E-G). OS-1 peptide⁶⁸ did not alter the effect of S100A8/A9 on platelets while inhibited VWF-induced platelet agglutination in the presence of ristocetin (supplemental Figure 4C-D, H-J). The effect of S100A8/A9 was not altered by increasing the concentrations of OS-1 (supplemental Figure 4H-J). Priming of platelets with S100A8/A9 did not induce platelet agglutination in the presence of VWF (Figure 6E-F), however, S100A8/A9 potentiated VWF-mediated platelet agglutination in the presence of ristocetin (Figure 6E,G). These results show that S100A8/A9 binds to GPIIb, overlapping with VWF-binding sites, and it potentiates VWF-dependent platelet agglutination.

GPIIb is the main receptor for S100A8/A9 on human platelets To confirm that GPIIb is the main receptor for S100A8/A9 on human platelets, platelet activation by S100A8/A9 was assessed in the presence of recombinant soluble GPIIb (His-17-Leu505) (rGPIIb) as a competitive strategy. Human washed platelets failed to respond to S100A8/A9 in the presence of equimolar concentrations of rGPIIb (1.7 μ M) (Figure 7A-I). The inhibitory effect was observed for P-selectin upregulation (Figure 7A-C), PS exposure (Figure 7D-F), and GPIIb/IIIa activation (Figure 7G-H). Furthermore, rGPIIb inhibited the formation of PS-positive MV (Figure 7I).

The key role for GPIIb was confirmed using platelets isolated from a patient with Bernard-Soulier syndrome (deficiency in GPIIb-V-IX complex). The patient has a mutation in *GP9* gene resulting in a defect in GPIIb/IX/V complex and the absence of GPIIb expression from platelets (detailed in Supplemental data). Platelets from this patient failed to respond to S100A8/A9, whereas the response to CRP was normal (Figure 7J-L). S100A8/A9 did not induce P-selectin expression, GPIIb/IIIa activation, or PS exposure (Figure 7J-L). These results confirm that GPIIb is the main receptor regulating S100A8/A9-mediated human and mouse platelet activation inducing P-selectin expression, GPIIb/IIIa activation, and the formation of procoagulant platelets and platelet-derived PS-positive MVs.

Discussion

In this study, we identified S100A8/A9-GPIIb axis as a novel mechanism triggering the formation of procoagulant platelets, independent of platelet aggregation. We show that (1) S100A8/A9 levels are increased in the plasma of patients with COVID-19 and that sustained high levels correlate with adverse outcome; (2) staining of lung autopsies from fatal COVID-19 cases showed a deposition of S100A8/A9 on lung vessel walls, in neutrophils, and a population of CD42b-positive cells; (3) immobilized recombinant heterodimeric S100A8/A9 accelerated fibrin generation at venous shear rate; (4) S100A8/A9 heterodimer but not S100A8 or S100A9 monomers/homodimers induced a slow alpha granule secretion, an increase in intracellular Ca^{2+} and a rapid exposure of PS; (5) S100A8/A9 failed to induce fibrinogen

binding and platelet aggregation, despite GPIIb/IIIa activation; (6) S100A8/A9-mediated formation of procoagulant platelet occurred independently of S100A8/A9 classic receptors RAGE and TLR-4, but it was mediated by the platelet adhesion receptor GPIIb with a supporting role for CD36; and (7) S100A8/A9-mediated platelet activation is resistant to classic antiplatelet drug targeting cyclo-oxygenase and P2Y12.

Platelet activation and high levels of S100A8/A9 are observed in many thromboinflammatory diseases including MI, DVT, and infections such as COVID-19,^{25,33,34,69,70} and these parameters correlate with thrombotic complications. The presence of procoagulant platelets with high cytosolic Ca^{2+} and PS levels were observed in patients with COVID-19, and these levels correlated with increased organ failure assessment score and D-dimer levels and were more pronounced in patients with thrombotic complications.^{11,71} Moreover, procoagulant MVs are detected even in nonsevere forms of the disease.^{72,73} The formation of procoagulant platelets in patients with COVID-19 is partially antibody driven,⁷¹ however, alternative pathways might be involved, particularly in the early days after SARS-CoV-2 infection. In accordance to previous reports,^{25,26,74} we found elevated levels of S100A8/A9 in patients with COVID-19. The levels of S100A8/A9 were higher in severely ill patients and sustained high levels of S100A8/A9 over the first week of monitoring were observed in nonsurvivors and associated with worse prognosis. In lung autopsies from fatal COVID-19 cases, S100A8/A9 was found mainly in neutrophils, a population of CD42b-positive cells, and on the vessel wall. NETosis, neutrophil necrosis, and platelet activation were shown to induce S100A8/A9 release, and these levels were further enriched in pathologic conditions.^{28,75} Platelets isolated from COVID-19 patients are enriched in S100A8 and S100A9 mRNA and platelet releasate from COVID-19 patients induces endothelial cell activation in vitro in a CD36-dependent manner.²⁸ In our cohort, S100A9 was detected in platelets, whereas the presence of the S100A8/A9 heterodimer was less pronounced. It was recently shown that neutrophils transfer S100A8 and S100A9 to platelets during NETosis or necrosis and the abundance of S100A8/A9 in platelets depends on neutrophil count in patients with ST-elevation MI.⁶⁹ Whether platelets contain S100A8 and S100A9 as monomer/homodimers rather than heterodimers with distinct proinflammatory and prothrombotic functions requires further investigation.

Because S100A8/A9 deposition on venules supports immune cell recruitment and transmigration,²⁹ we assessed its capacity to induce platelet activation and thrombosis at venous shear rate. Although immobilized S100A8/A9 induced platelet adhesion, an increase in intracellular Ca^{2+} , the expression of P-selectin, PS-positive platelets, and MVs, S100A8/A9 alone did not support platelet aggregation and significant fibrin generation at venous shear rate. However, co-immobilization of S100A8/A9 with collagen accelerated fibrin generation in recalcified blood, which was associated with early recruitment of PS-positive platelets. This procoagulant effect was not observed in PRP, because addition of soluble S100A8/A9 in PRP did not support thrombin generation. These data suggest that immobilized S100A8/A9 rather than plasma-soluble S100A8/A9 represents a potent prothrombotic danger signal supporting thrombosis in healthy donors. It is tempting to speculate that S100A8/A9 deposition on the vasculature in

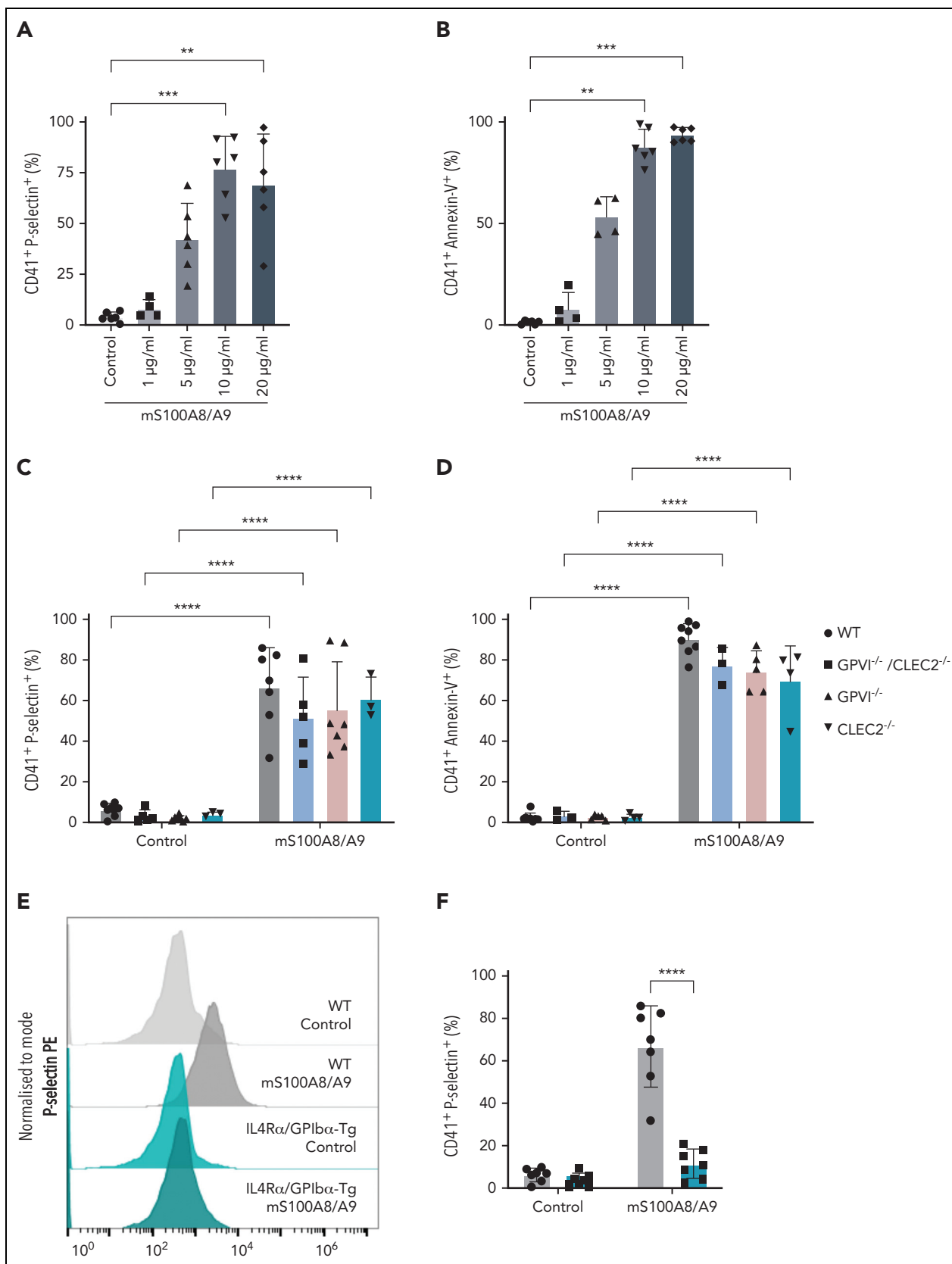


Figure 5. Murine S100A8/A9 activates mouse platelets through GPIIb and CD36. Washed murine platelets (10^6 platelets/condition) were incubated with different doses of recombinant mouse S100A8/A9 for 30 minutes at 37°C. Platelet activation was determined by flow cytometry using (A) anti-P-selectin antibody and (B) annexin-V binding. (C-K) Washed platelets isolated from WT, GPVI (GPVI^{-/-}), CLEC-2 (CLEC2^{-/-}), GPVI/CLEC-2 knock-out (GPVI^{-/-}/CLEC2^{-/-}), or GPIIb^{-/-} mice (IL4R/GPIIbα-Tg mice) were incubated with S100A8/A9 (10 μg/mL) for 30 minutes at 37°C. The percentage of platelets positive for P-selectin, GPIIb/IIIa activation (JON/A), and annexin-V binding were

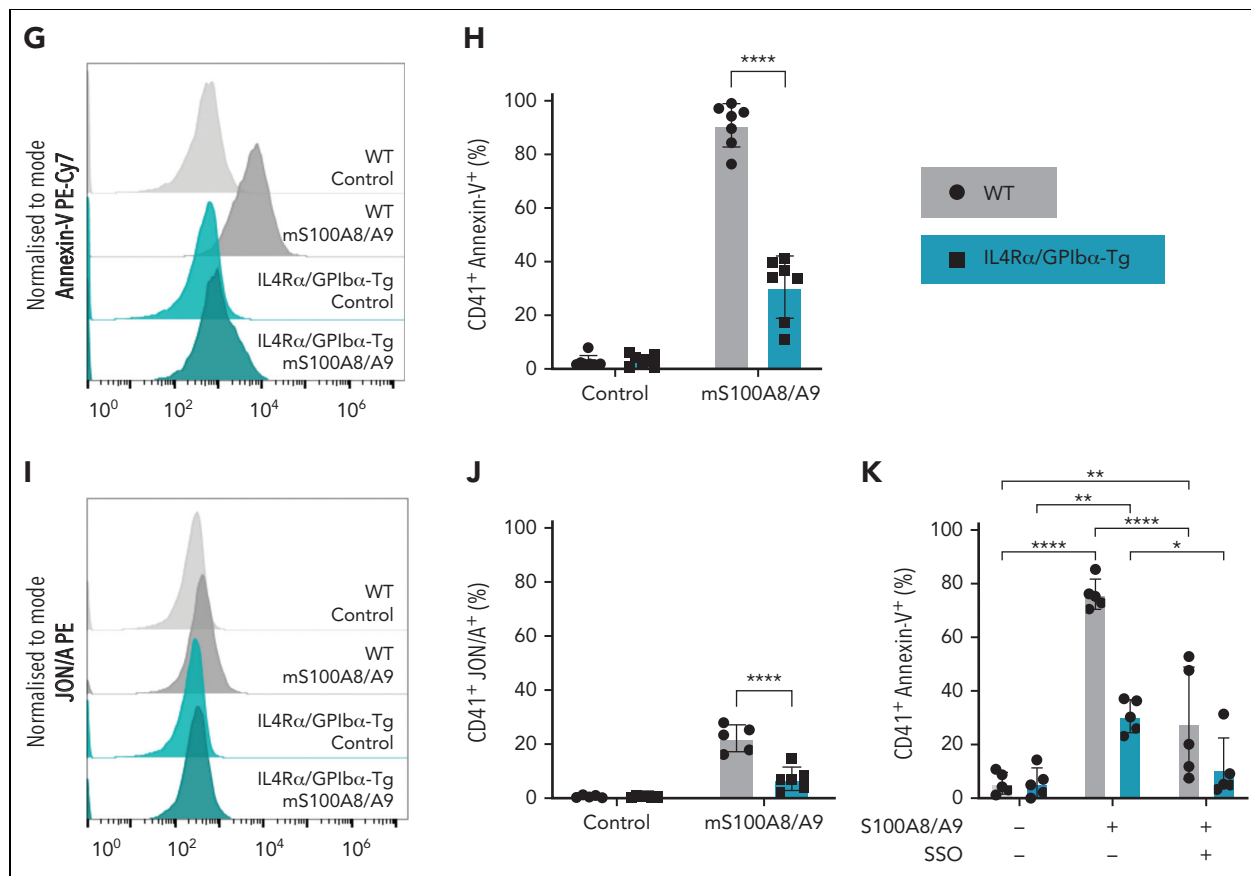


Figure 5 (continued) measured by flow cytometry. Data are shown as percentage platelets (CD41⁺) positive for different markers. (K) Platelets isolated from WT or IL4R/GPIb α -Tg mice were pretreated with SSO (25 μ M) before addition of S100A8/A9 (10 μ g/mL) for 30 minutes at 37°C, and annexin-V binding was assessed by flow cytometry. The statistical significance was analyzed using nonparametric test (Kruskal-Wallis test) (A-B), ordinary two-way ANOVA with Sidak's multiple comparison test (C,D,F,H,J), and two-way ANOVA with Tukey's multiple comparison test (K). Data are shown as mean \pm SD. **P* < .05, ***P* < .005, *****P* < .001.

COVID-19 patients contributes to the formation of fibrin-rich thrombi.

The early recruitment of PS-positive platelets and subsequent fibrin generation on immobilized S100A8/A9 suggest the formation of procoagulant platelets. The formation of procoagulant platelets in vitro is classically studied after co-stimulation of platelets with collagen and thrombin or with Ca²⁺ ionophore A23187, which can lead to the formation of 2 types of procoagulant platelets, with distinct properties.⁶⁰ The first population is associated with a sustained level of intracellular Ca²⁺, depolarized mitochondrial membrane, and inactivated GPIIb/IIIa with low capacity to aggregate. The second population retains mitochondrial membrane potential with intracellular Ca²⁺ levels returning to normal, active GPIIb/IIIa, and high aggregation properties.^{60,76-79} S100A8/A9-induced procoagulant platelets share common features of both populations, which might be due to distinct signaling pathways downstream of S100A8/A9 binding to platelets. S100A8/A9, but not S100A8 or S100A9 alone, induced procoagulant platelets with activated GPIIb/IIIa. However, S100A8/A9-activated platelets failed to bind fibrinogen and to induce platelet aggregation, suggesting the presence of a novel prothrombotic mechanism associated

with GPIIb/IIIa activation but independent of platelet aggregation. We further identified GPIb α as the main receptor for S100A8/A9 supporting the formation of procoagulant platelets, both in mice and humans. GPIb α has multiple extracellular agonists including VWF, thrombin, P-selectin,⁸⁰ and MAC-1,⁸¹ and these interactions regulate thrombosis and inflammation.⁸² Using antibodies recognizing epitopes on GPIb α involved in VWF binding, we further show that blocking Leu36-Gln59 region with AK2 antibody⁶⁶ or the anionic/sulfated tyrosine region (Tyr276-Glu282) with SZ2 antibody⁵⁷ decreased S100A8/A9-induced PS exposure and GPIIb/IIIa activation. These results suggest that S100A8/A9 effect on platelets is regulated by at least 2 different sites on GPIb α . It is possible that S100A8/A9 binding to these epitopes further affects the engagement of GPIb α with VWF, P-selectin, and MAC-1 altering immune cell activation and recruitment, independent of thrombosis. The anionic/sulfated region on GPIb α , with its high negative charge and sulfate groups, shares similarities with heparin, which can bind with high affinity to S100A8/A9.⁴⁶ Whether S100A8/A9 binding to this heparin-like sequence on GPIb α induces the formation of procoagulant platelets requires further investigation. S100A8/A9 binding to platelets further potentiates VWF-dependent platelet agglutination in the

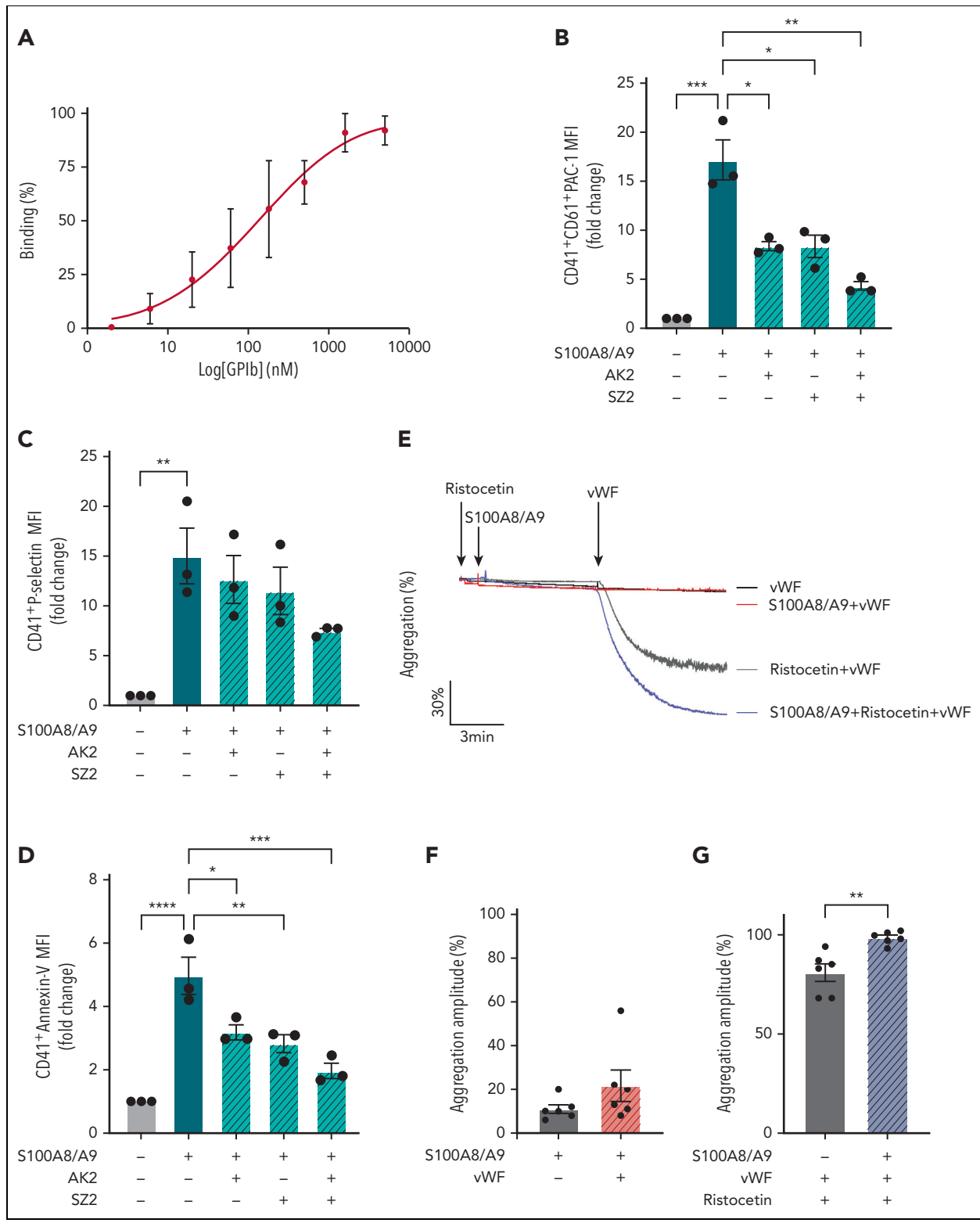


Figure 6. GPIIb/IIIa binds to S100A8/A9 and increases VWF-dependent platelet aggregation. (A) Binding of rGPIIb to immobilized S100A8/A9. Data presented as mean \pm SEM (n = 3). (B-D) Washed human platelets (10^6 /condition) were preincubated with or without AK2 Ab (40 μ g/mL), SZ2 (40 μ g/mL), or both for 10 minutes at 37°C and then stimulated with S100A8/A9 (20 μ g/mL) for 30 minutes at 37°C. Platelet activation was determined by flow cytometry using (B) anti-CD41/CD61 PAC-1 antibody, (C) anti-P-selectin antibody, and (D) annexin-V binding. Data are shown as MFI of treated platelets over control (unstimulated) for different markers. (E-G) Ristocetin-induced platelet aggregation was assessed by addition of VWF (1 μ g/mL) and ristocetin (1.5 mg/mL) to washed platelets. Platelets were primed with S100A8/A9 and ristocetin for 6 minutes before addition of VWF. Platelet aggregation was monitored for 6 minutes after VWF addition (n = 6). (E) Representative trace. Data are shown as mean \pm SEM. The statistical significance was analyzed using ordinary one-way ANOVA (B-D) and nonparametric Mann-Whitney t test (Kruskal-Wallis test) (F-G). **P* < .05, ***P* < .01, ****P* < .001, *****P* < .0001.

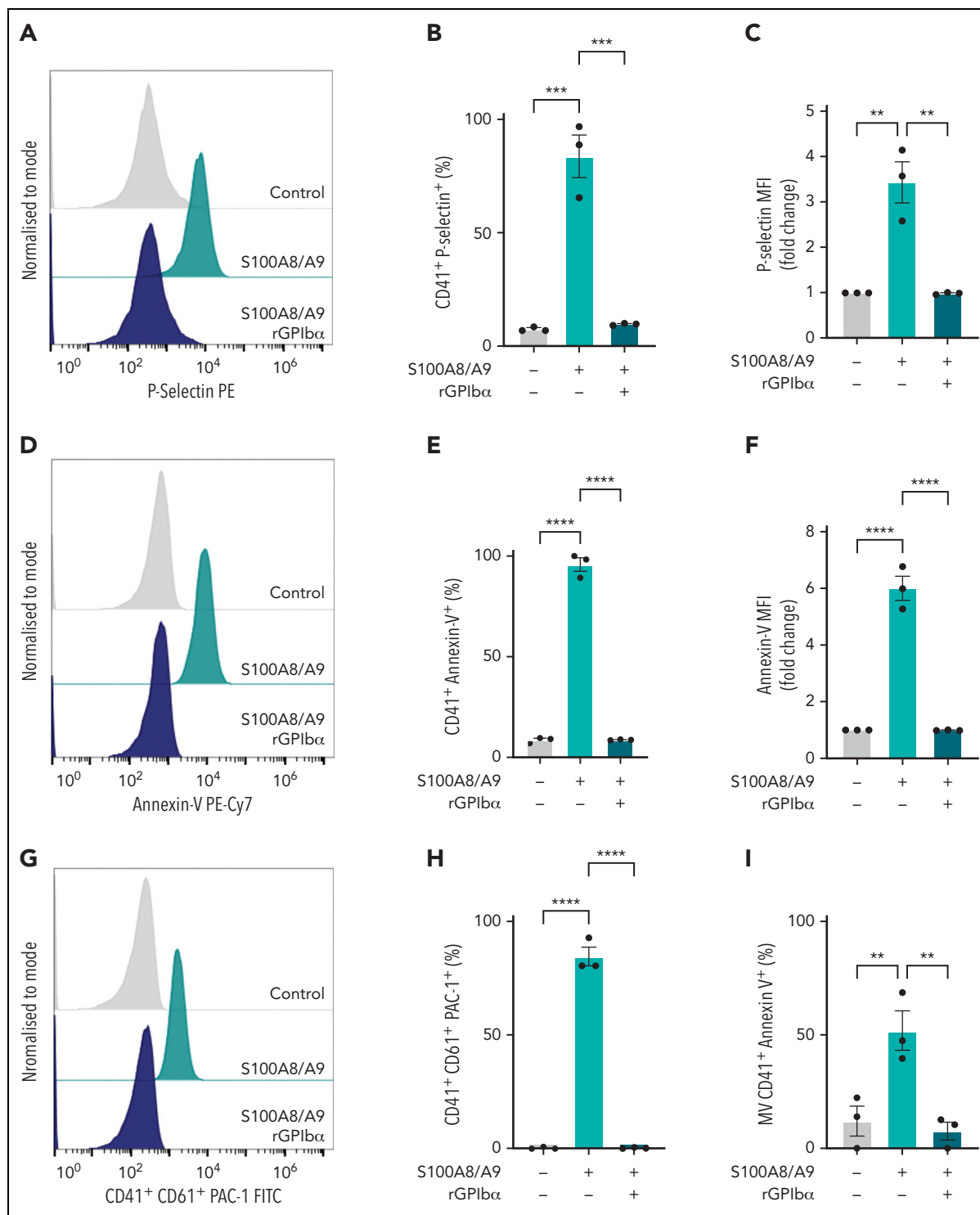


Figure 7. Recombinant human GPIIb/IIIa blocks platelet response to S100A8/A9, whereas Bernard-Soulier syndrome platelets failed to respond to S100A8/A9. Washed human platelets (10^6 platelets/condition) were incubated with S100A8/A9 (40 μ g/mL) in the absence or presence of recombinant human GPIIb/IIIa (rGPIIb/IIIa; 1.7 μ M) for 30 minutes at 37°C ($n = 3$). Platelet activation was assessed by flow cytometry using (A-C) anti-P-selectin, (D-F) PS exposure using annexin-V, and (G-I) GPIIb/IIIa activation using PAC-1 antibody. Human washed platelets from a healthy donor or a Bernard-Soulier syndrome patient were incubated with S100A8/A9 (20 and 40 μ g/mL) for 30 minutes at 37°C (J-L). CRP (10 μ g/mL) was used as positive control. (J) GPIIb/IIIa activation, (K) P-selectin, and (L) PS exposure were measured. The statistical significance was analyzed using one-way ANOVA. Data presented as mean \pm SEM. * $P < .05$, ** $P < .005$, *** $P < .001$, **** $P < .0001$.

presence of ristocetin, suggesting synergy between S100A8/A9 and VWF. This can be further modulated by CD36 because blockade of the receptor with SSO reduces GPIIb/IIIa activation and PS exposure. Indeed, CD36 was previously shown to

partially reduce S100A8/A9-induced thrombosis in mouse models of DVT, photochemical-induced carotid injury, and laser-induced injury to the cremaster microcirculation.^{27,34} Our data support the contribution of CD36 to platelet GPIIb/IIIa

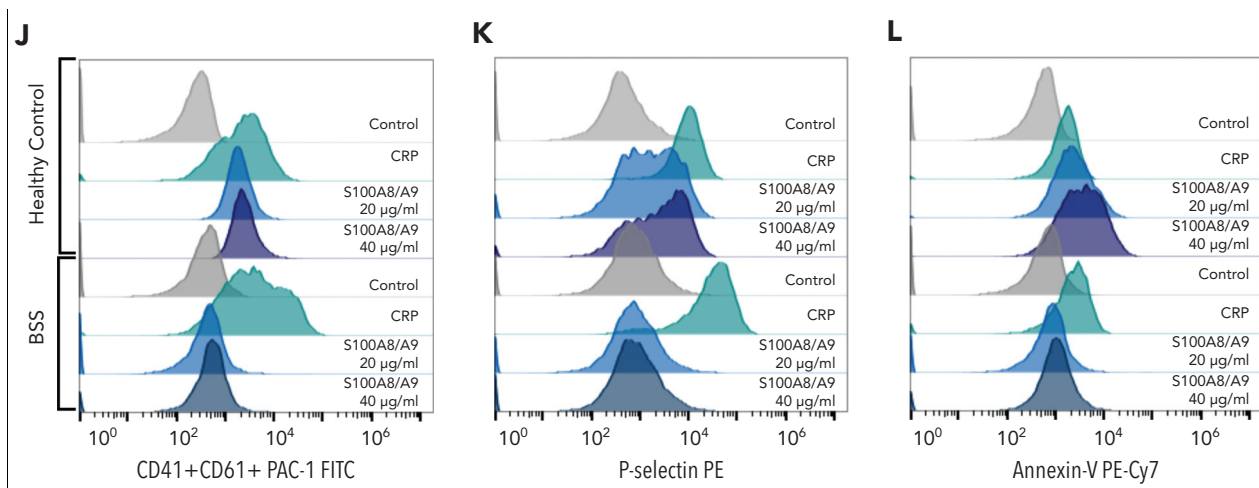


Figure 7. (continued)

activation and PS exposure without affecting P-selectin expression. It is likely that the initial interaction occurs through GPIIb α with crosstalk between GPIIb α and CD36, essential for platelet activation.⁸³

In conclusion, our study identified for the first time the S100A8/A9-GPIIb α axis as a novel immune-driven pathway for the formation of procoagulant platelets accelerating fibrin generation. Despite GPIIb/IIIa activation, platelets failed to bind to fibrinogen, suggesting that this mechanism of thrombosis is independent of platelet aggregation. Existing drugs can block distinct pathways, with Syk inhibitors reducing P-selectin expression on platelets and subsequent platelet-neutrophil aggregates. However, inhibition of GPIIb α alone or in conjunction with CD36 is essential to limit PS exposure and GPIIb/IIIa activation. Because this novel mechanism is resistant to classic, emerging antiplatelet or anti-S100A8/A9 drugs targeting TLR4 and RAGE, this study supports the need for the development of novel therapies to limit the formation of procoagulant platelets in thromboinflammatory diseases associated with the release of S100A8/A9, such as COVID-19.

Acknowledgments

The authors thank Beata Grygielska for genotyping mice and University of Birmingham Enterprise Ltd or the translational Research Team for their support.

J.R. holds a British Heart Foundation (BHF) Intermediate Fellowship (FS/IBSRF/20/25039). This research was partially supported by a BHF project grant (PG/21/10737), the BHF Accelerator Award (AA/18/2/34218), UK Spine Knowledge exchange (R78606/CN003), and the Medical Research Council (Grant Number MC_PC_19029) for J.R. M.C. is supported by the Wellcome Trust 4 Year PhD studentship program on Mechanisms of Inflammatory Disease (204951). A.A. is supported by the Austrian Science Fund (P32064 and P34783). G.P. is supported by a Birmingham-Maastricht studentship. S.P.W. holds a BHF Chair (CH03/003). A.O.K. is a Henry Wellcome fellow (218649/Z/19/Z). N.J.M. is supported by University of Aberdeen Development Trust and National Health Service Grampian Endowment funds (COV19-004 and 20/021). A.J.I. holds a Birmingham fellowship.

Authorship

Contribution: M.C. designed and performed experiments, collected and analyzed data, and wrote the manuscript; W.C.S., G.P., M.J.S., J.P., J.C.C., J.B., J.S.R., Z.Z., and A.S. performed experiments and analyzed data; J.H.B. and A.O.K. analyzed data; M.P., N.S.P., P.L.R.N., P.H., A.J.I., G.E.R., S.P.W., and M.R.T. provided key reagents and contributed to data analysis; N.J.M. and A.A. provided key reagents and supported research analysis; J.R. designed research and experiments, performed experiments, collected and analyzed data, and wrote the manuscript; and all authors read and approved the paper.

Conflict-of-interest disclosure: This work is protected by UoB patent (Patent Application Number: PCT/GB2022/052007). The authors declare no competing financial interests.

ORCID profiles: M.C., 0000-0002-5622-6565; W.C.S., 0000-0003-0550-4120; G.P., 0000-0002-0516-4261; J.S.R., 0000-0003-3247-9186; J.B., 0000-0002-2992-0578; A.S., 0000-0001-7166-438X; J.P., 0000-0001-9950-7992; J.C.C., 0000-0002-1912-7816; Z.Z., 0000-0003-0896-1677; M.J.S., 0000-0002-3824-8808; J.H.B., 0000-0003-4442-5767; N.S.P., 0000-0002-3187-2130; A.O.K., 0000-0003-0825-3179; M.P., 0000-0002-6324-661X; P.H., 0000-0003-4610-8909; A.J.I., 0000-0002-3224-3651; S.P.W., 0000-0002-7846-7423; N.J.M., 0000-0002-7452-0813; J.R., 0000-0003-0499-6880.

Correspondence: Julie Rayes, Institute of Cardiovascular Sciences, College of Medical and Dental Sciences, University of Birmingham, Birmingham, B15 2TT, United Kingdom; email: j.rayes@bham.ac.uk.

Footnotes

Submitted 29 November 2021; accepted 9 August 2022; prepublshed online on *Blood* First Edition 26 August 2022. <https://doi.org/10.1182/blood.2021014966>.

Data are available on request from the corresponding author, Julie Rayes (j.rayes@bham.ac.uk).

The online version of this article contains a data supplement.

The publication costs of this article were defrayed in part by page charge payment. Therefore, and solely to indicate this fact, this article is hereby marked "advertisement" in accordance with 18 USC section 1734.

REFERENCES

- Russwurm S, Vickers J, Meier-Hellmann A, et al. Platelet and leukocyte activation correlate with the severity of septic organ dysfunction. *Shock*. 2002;17(4):263-268.
- Nicolai L, Massberg S. Platelets as key players in inflammation and infection. *Curr Opin Hematol*. 2020;27(1):34-40.
- Lievens D, Zernecke A, Seijkens T, et al. Platelet CD40L mediates thrombotic and inflammatory processes in atherosclerosis. *Blood*. 2010;116(20):4317-4327.
- Zhou J, Xu E, Shao K, et al. Circulating platelet-neutrophil aggregates as risk factor for deep venous thrombosis. *Clin Chem Lab Med*. 2019;57(5):707-715.
- Marquardt L, Anders C, Bugge F, et al. Leukocyte-platelet aggregates in acute and subacute ischemic stroke. *Cerebrovasc Dis*. 2009;28(3):276-282.
- Ren F, Mu N, Zhang X, et al. Increased platelet-leukocyte aggregates are associated with myocardial no-reflow in patients with ST elevation myocardial infarction. *Am J Med Sci*. 2016;352(3):261-266.
- Schrottmaier WC, Mussbacher M, Salzmann M, Assinger A. Platelet-leukocyte interplay during vascular disease. *Atherosclerosis*. 2020;307:109-120.
- Gawaz M, Fateh-moghadam S, Pilz G, Gurland H-J, Werdan K. Platelet activation and interaction with leukocytes in patients with sepsis or multiple organ failure. *Eur J Clin Invest*. 1995;25(11):843-851.
- Koupenova M, Corkrey HA, Vitseva O, et al. The role of platelets in mediating a response to human influenza infection. *Nat Commun*. 2019;10(1):1-18.
- Hottz ED, Azevedo-Quintanilha IG, Palhinha L, et al. Platelet activation and platelet-monocyte aggregate formation trigger tissue factor expression in patients with severe COVID-19. *Blood*. 2020;136(11):1330-1341.
- Khattab MH, Prodan CI, Vincent AS, et al. Increased procoagulant platelet levels are predictive of death in COVID-19. *GeroScience*. 2021;43(4):2055-2065.
- Yatim N, Boussier J, Chocron R, et al. Platelet activation in critically ill COVID-19 patients. *Ann Intensive Care*. 2021;11(1):1-12.
- Rondina MT, Carlisle M, Fraughton T, et al. Platelet-monocyte aggregate formation and mortality risk in older patients with severe sepsis and septic shock. *J Gerontol Ser A*. 2015;70(2):225-231.
- Vulliamy P, Gillespie S, Armstrong PC, Allan HE, Warner TD, Brohi K. Histone H4 induces platelet ballooning and microparticle release during trauma hemorrhage. *Proc Natl Acad Sci U S A*. 2019;116(35):17444-17449.
- Khismatullin RR, Ponomareva AA, Nagaswami C, et al. Pathology of lung-specific thrombosis and inflammation in COVID-19. *J Thromb Haemost*. 2021;19(12):3062-3072.
- Loeffen R, Godschalk TC, Oerle R van, et al. The hypercoagulable profile of patients with stent thrombosis. *Heart*. 2015;101(14):1126-1132.
- Morel O, Jesel L, Freyssinet J, Toti F. Elevated levels of procoagulant microparticles in a patient with myocardial infarction, antiphospholipid antibodies and multifocal cardiac thrombosis. *Thromb J*. 2005;3(1):1-5.
- Shannon O. The role of platelets in sepsis. *Res Pract Thromb Haemost*. 2021;5(1):27-37.
- Kerris EWJ, Hoptay C, Calderon T, Freishtat RJ. Platelets and platelet extracellular vesicles in hemostasis and sepsis. *J Invest Med*. 2020;68(4):813-820.
- Lukasik M, Rozalski M, Luzak B, et al. Enhanced platelet-derived microparticle formation is associated with carotid atherosclerosis in convalescent stroke patients. *Platelets*. 2013;24(1):63-70.
- Prodan CI, Stoner JA, Cowan LD, Dale GL. Higher coated-platelet levels are associated with stroke recurrence following nonlacunar brain infarction. *J Cerebr Blood Flow Metabol*. 2013;33(2):287-292.
- Prodan CI, Vincent AS, Dale GL. Coated-platelet levels are elevated in patients with transient ischemic attack. *Transl Res*. 2011;158(1):71-75.
- Gould TJ, Lysov Z, Liaw PC. Extracellular DNA and histones: double-edged swords in immunothrombosis. *J Thromb Haemost*. 2015;13(5):S82-S91.
- Kapoor S, Opneja A, Najak L. The role of neutrophils in thrombosis. *Thromb Res*. 2018;170:87-96.
- Guo Q, Zhao Y, Li J, et al. Induction of alarmin S100A8/A9 mediates activation of aberrant neutrophils in the pathogenesis of COVID-19. *Cell Host Microbe*. 2021;29(2):222-235.e4.
- Mahler M, Meroni P-L, Infantino M, Buhler KA, Fritzlir MJ. Circulating Calprotectin as a Biomarker of COVID-19 Severity. *Expert Rev Clin Immunol*. 2021;17(5):431-443.
- Wang Y, Fang C, Gao H, et al. Platelet-derived S100 family member myeloid-related protein-14 regulates thrombosis. *J Clin Invest*. 2014;124(5):2160-2171.
- Barrett TJ, Cornwell M, Myndzar K, et al. Platelets amplify endotheliopathy in COVID-19. *Sci Adv*. 2021;7(37):eabh-2434.
- Hogg N, Allen C, Edgeworth J. Monoclonal antibody 5.5 reacts with p8,14, a myeloid molecule associated with some vascular endothelium. *Eur J Immunol*. 1989;19(6):1053-1061.
- Frangogiannis NG. S100A8/A9 as a therapeutic target in myocardial infarction: cellular mechanisms, molecular interactions, and translational challenges. *Eur Heart J*. 2019;40(32):2724-2726.
- Schiopu A, Marinkovic G, DeCamp L, et al. The S100A8/A9 alarmin stimulates myeloid cell response and promotes cardiac repair after myocardial infarction. *Atherosclerosis*. 2018;275:e7.
- Schiopu A, Cotoi OS. S100A8 and S100A9: DAMPs at the crossroads between innate immunity, traditional risk factors, and cardiovascular disease. *Mediat Inflamm*. 2013;2013:828354.
- Dubois C, Marcé D, Faivre V, et al. High plasma level of S100A8/S100A9 and S100A12 at admission indicates a higher risk of death in septic shock patients. *Sci Rep*. 2019;9(1):1-7.
- Wang Y, Gao H, Kessinger CW, et al. Myeloid-related protein-14 regulates deep vein thrombosis. *JCI Insight*. 2017;2(11).
- Geven EJW, van den Bosch MHJ, Di Ceglie I, et al. S100A8/A9, a potent serum and molecular imaging biomarker for synovial inflammation and joint destruction in seronegative experimental arthritis. *Arthritis Res Ther*. 2016;18(1):1-12.
- Okada K, Okabe M, Kimura Y, Itoh H, Ikemoto M. Serum S100A8/A9 as a potentially sensitive biomarker for inflammatory bowel disease. *Lab Med*. 2019;50(4):370-380.
- Müller I, Vogl T, Kühl U, et al. Serum alarmin S100A8/S100A9 levels and its potential role as biomarker in myocarditis. *ESC Heart Fail*. 2020;7(4):1442-1451.
- Wang S, Song R, Wang Z, et al. S100A8/A9 in Inflammation. *Front Immunol*. 2018;9:1298.
- Zhong X, Xie F, Chen L, Liu Z, Wang Q. S100A8 and S100A9 promote endothelial cell activation through the RAGE-mediated mammalian target of rapamycin complex 2 pathway. *Mol Med Rep*. 2020;22(6):5293-5303.
- Edgeworth J, Gorman M, Bennett R, Freemont P, Hogg N. Identification of p8,14 as a highly abundant heterodimeric calcium binding protein complex of myeloid cells. *J Biol Chem*. 1991;266(12):7706-7713.
- Hessian PA, Edgeworth J, Hogg N. MRP-8 and MRP-14, two abundant Ca²⁺-binding proteins of neutrophils and monocytes. *J Leukoc Biol*. 1993;53(2):197-204.
- Chen B, Miller AL, Rebelatto M, et al. S100A9 induced inflammatory responses are mediated by distinct damage associated molecular patterns (DAMP) receptors in vitro and in vivo. *PLoS One*. 2015;10(2):e0115828.
- Fuentes E, Rojas A, Palomo I. Role of multiligand/RAGE axis in platelet activation. *Thromb Res*. 2014;133(3):308-314.
- Ghosh A, Murugesan G, Chen K, et al. Platelet CD36 surface expression levels affect functional responses to oxidized LDL and are associated with inheritance of specific genetic polymorphisms. *Blood*. 2011;117(23):6355-6366.
- Assinger A, Schrottmaier WC, Salzmann M, Rayes J. Platelets in sepsis: an update on

- experimental models and clinical data. *Front Immunol.* 2019;10:1687.
46. Robinson MJ, Tessier P, Poulsom R, Hogg N. The S100 family heterodimer, MRP-8/14, binds with high affinity to heparin and heparan sulfate glycosaminoglycans on endothelial cells. *J Biol Chem.* 2002;277(5):3658-3665.
 47. Kerkhoff C, Sorg C, Tandon NN, Nacken W. Interaction of S100A8/S100A9-arachidonic acid complexes with the scavenger receptor CD36 may facilitate fatty acid uptake by endothelial cells. *Biochemistry.* 2001;40(1):241-248.
 48. Mussbacher M, Schrottmaier WC, Salzmann M, et al. Optimized plasma preparation is essential to monitor platelet-stored molecules in humans. *PLoS One.* 2017;12(12):e0188921.
 49. Khan AO, Reyat JS, Hill H, et al. Preferential uptake of SARS-CoV-2 by pericytes potentiates vascular damage and permeability in an organoid model of the microvasculature [published online ahead of print 16 June 2022]. *Cardiovasc Res.* <https://doi.org/10.1093/cvr/cvac097>
 50. Futami J, Atago Y, Azuma A, et al. An efficient method for the preparation of preferentially heterodimerized recombinant S100A8/A9 coexpressed in *Escherichia coli*. *Biochem Biophys Reports.* 2016;6:94.
 51. Hughes CE, Pollitt AY, Mori J, et al. CLEC-2 activates Syk through dimerization. *Blood.* 2010;115(14):2947-2955.
 52. Nicolson PLR, Hughes CE, Watson S, et al. Inhibition of Btk by Btk-specific concentrations of ibrutinib and acalabrutinib delays but does not block platelet aggregation mediated by glycoprotein VI. *Haematologica.* 2018;103(12):2097-2108.
 53. Zuo Y, Zuo M, Yalavarthi S, et al. Neutrophil extracellular traps and thrombosis in COVID-19. *J Thromb Thrombolysis.* 2020;51(2):446-453.
 54. Silvín A, Chapuis N, Dunsmore G, et al. Elevated calprotectin and abnormal myeloid cell subsets discriminate severe from mild COVID-19. *Cell.* 2020;182(6):1401-1418.
 55. Schrottmaier WC, Pirabe A, Pereyra D, et al. Platelets and antiplatelet medication in COVID-19-related thrombotic complications. *Front Cardiovasc Med.* 2022;8:802566.
 56. Schrottmaier WC, Pirabe A, Pereyra D, et al. Adverse outcome in COVID-19 is associated with an aggravating hypo-responsive platelet phenotype. *Front Cardiovasc Med.* 2021;8:795624.
 57. Schenten V, Plançon S, Jung N, et al. Secretion of the phosphorylated form of S100A9 from neutrophils is essential for the proinflammatory functions of extracellular S100A8/A9. *Front Immunol.* 2018;9:447.
 58. Shrivastava S, Chelluboina S, Jedge P, et al. Elevated levels of neutrophil activated proteins, alpha-defensins (DEFA1), calprotectin (S100A8/A9) and myeloperoxidase (MPO) are associated with disease severity in COVID-19 patients. *Front Cell Infect Microbiol.* 2021;11:751232.
 59. Chen L, Long X, Xu Q, et al. Elevated serum levels of S100A8/A9 and HMGB1 at hospital admission are correlated with inferior clinical outcomes in COVID-19 patients. *Cell Mol Immunol.* 2020;17(9):992-994.
 60. Topalov NN, Yakimenko AO, Canault M, et al. Two types of procoagulant platelets are formed upon physiological activation and are controlled by integrin $\alpha\text{IIb}\beta\text{3}$. *Arterioscler Thromb Vasc Biol.* 2012;32(10):2475-2483.
 61. Yang M, Cooley BC, Li W, et al. Platelet CD36 promotes thrombosis by activating redox sensor ERK5 in hyperlipidemic conditions. *Blood.* 2017;129(21):2917-2927.
 62. Ding N, Chen G, Hoffman R, et al. TLR4 regulates platelet function and contributes to coagulation abnormality and organ injury in hemorrhagic shock and resuscitation. *Circ Cardiovasc Genet.* 2014;7(5):615-624.
 63. I A, YC C, D T, et al. HMGB1 binds to activated platelets via the receptor for advanced glycation end products and is present in platelet rich human coronary artery thrombi. *Thromb Haemost.* 2015;114(5):994-1003.
 64. Ozaki Y, Suzuki-Inoue K, Inoue O. Platelet receptors activated via multimerization: glycoprotein VI, GPIb-IX-V, and CLEC-2. *J Thromb Haemost.* 2013;11(suppl 1):330-339.
 65. Heit B, Kim H, Cosío G, et al. Multimolecular signaling complexes enable Syk-mediated signaling of CD36 internalization. *Dev Cell.* 2013;24(4):372-383.
 66. Shen Y, Romo GM, Dong JF, et al. Requirement of leucine-rich repeats of glycoprotein (GP) Iba for shear-dependent and static binding of von Willebrand factor to the platelet membrane GP Iba-IX-V complex. *Blood.* 2000;95(3):903-910.
 67. Ward CM, Andrews RK, Smith AI, Berndt MC. Mocarhagin, a novel cobra venom metalloproteinase, cleaves the platelet von Willebrand Factor receptor glycoprotein Iba. Identification of the sulfated tyrosine/anionic sequence Tyr-276-Glu-282 of glycoprotein Iba as a binding site for von Willebrand Factor. *Biochemistry.* 1996;35(15):4929-4938.
 68. McEwan PA, Andrews RK, Emsley J. Glycoprotein Iba inhibitor complex structure reveals a combined steric and allosteric mechanism of von Willebrand factor antagonism. *Blood.* 2009;114(23):4883-4885.
 69. Joshi A, Schmidt LE, Burnap SA, et al. Neutrophil-derived protein S100A8/A9 alters the platelet proteome in acute myocardial infarction and is associated with changes in platelet reactivity. *Arterioscler Thromb Vasc Biol.* 2022;42(1):49-62.
 70. Mellett L, Khader SA. S100A8/A9 in COVID-19 pathogenesis: impact on clinical outcomes. *Cytokine Growth Factor Rev.* 2022;63:90-97.
 71. Althaus K, Marini I, Zlamal J, et al. Antibody-induced procoagulant platelets in severe COVID-19 infection. *Blood.* 2021;137(8):1061-1071.
 72. Wool GD, Miller JL. The impact of COVID-19 disease on platelets and coagulation. *Pathobiology.* 2021;88(1):15-27.
 73. Puhm F, Allaëys I, Lacasse E, et al. Platelet activation by SARS-CoV-2 implicates the release of active tissue factor by infected cells. *Blood Adv.* 2022;6(12):3593-3605.
 74. Canzano P, Brambilla M, Porro B, et al. Platelet and endothelial activation as potential mechanisms behind the thrombotic complications of COVID-19 patients. *JACC Basic Transl Sci.* 2021;6(3):202-218.
 75. Sprenkeler EGG, Zandstra J, van Kleef ND, et al. S100A8/A9 is a marker for the release of neutrophil extracellular traps and induces neutrophil activation. *Cells.* 2022;11(2):236.
 76. van Kruchten R, Mattheij NJ, Saunders C, et al. Both TMEM16F-dependent and TMEM16F-independent pathways contribute to phosphatidylserine exposure in platelet apoptosis and platelet activation. *Blood.* 2013;121(10):1850-1857.
 77. Choo HJ, Saafir TB, Mkumba L, Wagner MB, Jobe SM. Mitochondrial calcium and reactive oxygen species regulate agonist-initiated platelet phosphatidylserine exposure. *Arterioscler Thromb Vasc Biol.* 2012;32(12):2946-2955.
 78. Dale GL. Procoagulant platelets: further details but many more questions. *Arterioscler Thromb Vasc Biol.* 2017;37(9):1596-1597.
 79. Agbani EO, Poole AW. Procoagulant platelets: generation, function, and therapeutic targeting in thrombosis. *Blood.* 2017;130(20):2171-2179.
 80. Peyvandi F, Garagiola I, Baronciani L. Role of von Willebrand factor in the haemostasis. *Blood Transfus.* 2011;9(suppl 2):s3-8.
 81. Wang Y, Gao H, Shi C, et al. Leukocyte integrin Mac-1 regulates thrombosis via interaction with platelet GPIIb/IIIa. *Nat Commun.* 2017;8(1):1-16.
 82. Denorme F, Vanhoorelbeke K, De Meyer SF. von Willebrand factor and platelet glycoprotein Iba: a thromboinflammatory axis in stroke. *Front Immunol.* 2019;10:2884.
 83. Döhrmann M, Makhoul S, Gross K, et al. CD36-fibrin interaction propagates FXI-dependent thrombin generation of human platelets. *Faseb J.* 2020;34(7):9337-9357.

© 2022 by The American Society of Hematology. Licensed under Creative Commons Attribution-NonCommercial-NoDerivatives 4.0 International (CC BY-NC-ND 4.0), permitting only noncommercial, nonderivative use with attribution. All other rights reserved.